Geological Society of America
Reviews in Engineering Geology, Volume XI
1997

Hydroclimatological and paleohydrological context of extreme winter flooding in Arizona, 1993

P. Kyle House
Quaternary Sciences Center, Desert Research Institute, 7010 Dandini Boulevard, Reno, Nevada 89512
Katherine K. Hirschboeck
Laboratory of Tree-Ring Research, University of Arizona, Tucson, Arizona 85721

ABSTRACT

Extreme flooding in Arizona during the winter of 1993 resulted from a nearly optimal combination of flood-enhancing factors involving hydroclimatology, hydrometeorology, and physiography. The floods of January and February 1993 were the result of record precipitation from the passage of an unusually high number of winter storm fronts. These fronts moved across Arizona as part of an exceptionally active storm track that was located unusually far south. The number of individual storms that entered the region and the relative position of each storm track in relation to previous storms was reflected in a complex spatial and temporal distribution of flood peaks. An analysis of the hydroclimatic context of these floods supports a general conclusion that in Arizona, front-generated winter precipitation is most often the cause of extreme floods in large watersheds, even in basins that tend to experience their greatest frequency of flooding from other types of storms. A comparison of the 1993 floods with gauged, historical, and paleoflood data from Arizona indicates that, although many individual flood peaks were quite large, they were within the range of documented extreme flooding over the past 1,000+ yr. The 1993 flood scenario provides a convincing analogue for the climatic and hydrologic processes that must have operated to generate comparably large paleofloods, that is, abnormally high rainfall totals, repeated accumulation and melting of snow, and rain on snow. Such conditions are initiated and perpetuated by a persistent winter circulation anomaly in the North Pacific Ocean that repeatedly steers alternately warm and cold storms into the region along a southerly displaced storm track. This scenario is enhanced by an active subtropical jet stream, common during El Niño–Southern Oscillation periods.

INTRODUCTION

Record flood peaks occurred in many watersheds in Arizona during January and February 1993 (Smith et al., 1994). This widespread, high-magnitude flooding was the culmination of record amounts of precipitation (rain and snow) that fell statewide from a long succession of storms that began in early December 1992. Approximately 16 separate storms passed over the state over a three-month period that was characterized by anomalous and persistent patterns of atmospheric circulation (House, 1993; National Oceanic and Atmospheric Administration, 1992, 1993a, 1993b).

The 1993 flood sequence ranks as one of the most severe winter flooding episodes in Arizona history, possibly surpassed only by a similar episode in February 1891 (Patterson and Somers, 1966). In January and February 1993, record peak discharges were recorded at more than 35 stations (Fig. 1; Table 1). Unprecedented flow volumes and durations occurred, causing great concern for floodplain and reservoir management (Fig. 2). On several occasions in 1993, large volumes of inflow overtaxed reservoirs and

House, P. K., and Hirschboeck, K. K., 1997, Hydroclimatological and paleohydrological context of extreme winter flooding in Arizona, 1993, *in* Larson, R. A., and Slosson, J. E., eds., Storm-Induced Geologic Hazards: Case Histories from the 1992–1993 Winter in Southern California and Arizona: Boulder, Colorado, Geological Society of America Reviews in Engineering Geology, v. XI.

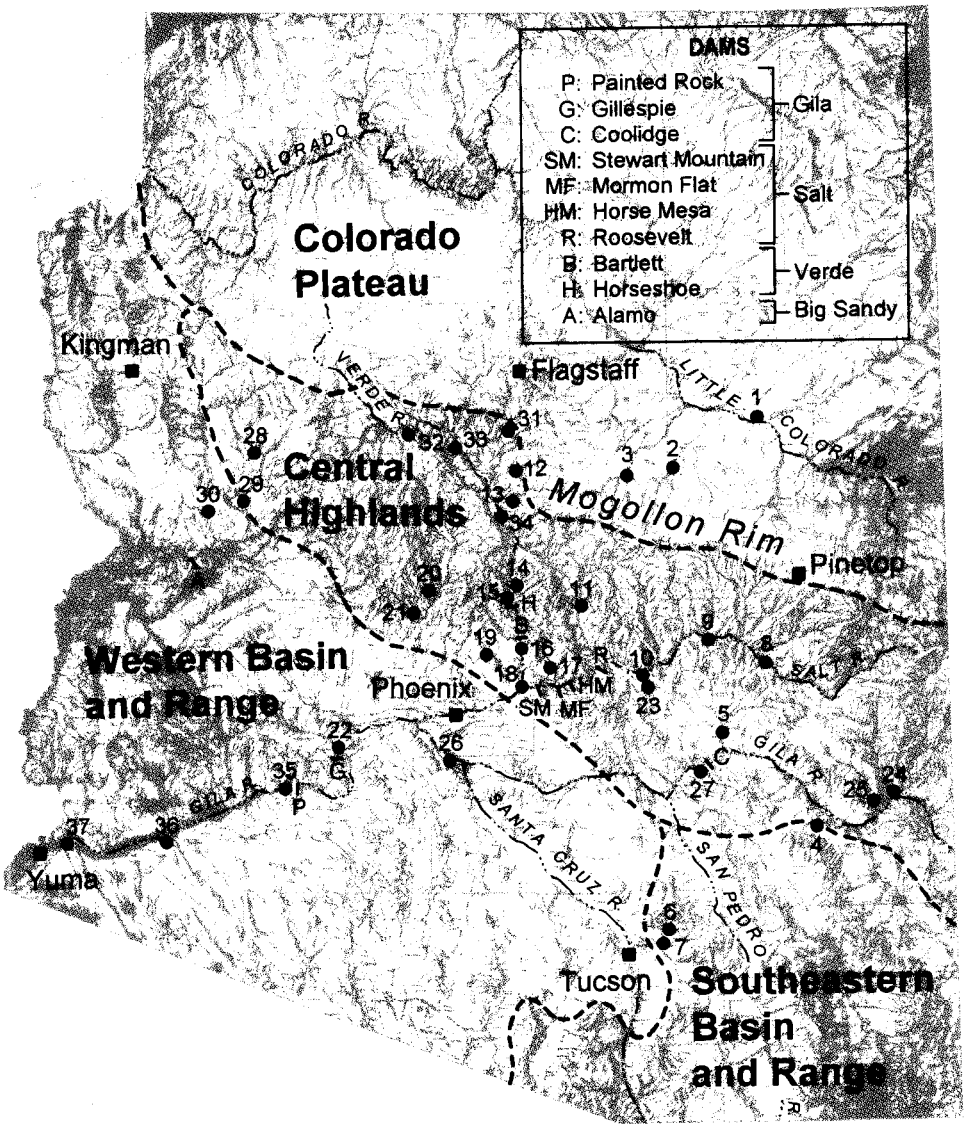

Figure 1. Map of Arizona showing physiographic regions discussed in text, sites of record floods at stations with at least 10 yr of record (numbered), the location of dams affected by flooding, and the location of sites mentioned in the text. Each record flood site is listed and described in Table 1.

forced massive, dramatic releases of flood runoff from many dams in Arizona (Fig. 3). The protracted flow durations downstream from the dams enhanced severe erosion of some floodplain areas. On the middle Gila River, for example, it has been shown that the protracted flow duration caused considerably greater channel and floodplain erosion than did a previous, shorter-lived flood with a greater instantaneous peak discharge (Huckleberry, 1994). The floodplain and channel erosion problem along much of the length of the Gila River during 1993 was probably compounded by sustained releases from flood control structures.

Total estimated damage from the 1993 floods exceeded $400 million, and total federal expenditures related to the flooding exceeded $220 million (U.S. Army Corps of Engineers, 1994). The Red Cross reported eight deaths and 112 injuries related to the floods. Federal disaster declarations were issued for 13 of 15 counties in Arizona, a direct reflection of the regional scope and severity of the flooding.

The goal of this chapter is to describe the 1993 Arizona flood sequence in the large-scale and long-term context of its hydroclimatic and hydrometeorologic origins and historical/prehistoric forerunners. In illustrating some of the more interesting flood phenomena, specific examples are presented that are assumed to have been reasonably representative of conditions throughout Arizona during the winter of 1992–1993.

THE CAUSES OF FLOODING

Flooding results from the interaction of three factors: (1) the short-term precipitation-delivering mechanisms that are the most immediate cause of the excessive runoff (*flood hydrometeorology*), (2) the large-scale atmospheric circulation pat-

TABLE 1. SUMMARY OF RECORD DISCHARGES IN ARIZONA, JANUARY AND FEBRUARY 1993*

Point	Site	USGS Number	Area (km^2)	Peak Discharge (m^3s^{-1})	Date 1993	Record Length	Prior Flood of Record: Peak Discharge (m^3s^{-1})	Prior Flood of Record: Date
1	Leroux Wash near Holbrook, AZ	9397100	2,095	240	8-Jan	13	215	24-Aug-92
2	Chevelon Creek near Winslow, AZ	9397500	702	699	8-Jan	35§	564	18-Dec-78
3	Clear Creek near Winslow, AZ†	9398500	821	824	8-Jan	42	558	18-Dec-78
4	Frye Creek near Thatcher, AZ	9460150	10	14	8-Jan	17§	3	24-Aug-92
5	San Carlos River near Peridot, AZ	9468500	2,657	1,552	8-Jan	68§	1,150	14-Mar-41
6	Sabino Creek near Tucson, AZ	9484000	92	365	8-Jan	63§	219	6-Sep-70
7	Tanque Verde Creek near Tucson, AZ	9484500	567	694	8-Jan	27§	360	18-Dec-78
8	Black River near Fort Apache, AZ	9490500	3,191	1,549	8-Jan	45§	1,252	2-Oct-83
9	Salt River near Chrysotile, AZ	9497500	7,379	2,169	8-Jan	71	1,994	18-Dec-78
10	Salt River near Roosevelt, AZ	9498500	11,153	4,050	8-Jan	82	3,313	14-Mar-41
11	Tonto Creek near Roosevelt, AZ	9499000	1,748	2,053	8-Jan	55	1,739	15-Feb-80
12	Wet Beaver Creek near Rimrock, AZ	9505200	287	453	8-Jan	34	309	19-Feb-80
13	West Clear Creek near Camp Verde, AZ	9505800	624	702	8-Jan	30	634	18-Dec-78
14	Wet Bottom Creek near Childs, AZ	9508300	94	209	8-Jan	28	193	19-Feb-80
15	Verde River below Tangle Creek, AZ	9508500	14,227	4,106	8-Jan	50	2,684	15-Feb-80
16	Verde River below Bartlett Dam, AZ†	9510000	15,032	3,115	8-Jan	56	2,860	2-Mar-78
17	Rock Creek near Sunflower, AZ	9510180	39	72	8-Jan	12§	54	22-Dec-65
18	Verde River near Scottsdale, AZ†	9511300	16,188	3,597	8-Jan	34	2,775	16-Feb-80
19	Cave Creek near Cave Creek, AZ	9512280	214	261	8-Jan	15	110	1-Mar-91
20	Boulder Creek near Rock Springs, AZ	9512830	98	283	8-Jan	10	91	1-Mar-91
21	Humbug Creek near Castle Hot Springs, AZ	9512860	155	170	8-Jan	12	91	1-Mar-91
22	Gila River at Gillespie Dam, AZ†	9518000	128,594	3,682	9-Jan	54	3,511	17-Feb-80
23	Pinal Creek near Globe, AZ	9498400	420	161	11-Jan	15	83	9-Jul-81
24	Eagle Creek near Morenci, AZ†	9447000	1,611	1,042	18-Jan	51	1,031	2-Oct-83
25	Bonita Creek near Morenci, AZ	9447800	782	552	18-Jan	14	549	2-Oct-83
26	Gila River near Laveen, AZ†	9479500	53,393	1,178	20-Jan	54	991	4-Oct-83
27	Gila River below Coolidge Dam, AZ†	9469500	33,375	830	21-Jan	67	142	6-Oct-83
28	Francis Creek near Bagdad, AZ	9424432	347	354	8-Feb	10	193	25-Aug-88
29	Burro Creek near Bagdad, AZ	9424447	1,557	1,566	8-Feb	14	866	3-Mar-83
30	Big Sandy River near Wikieup, AZ	9424450	7,076	1,946	8-Feb	29	1,090	20-Feb-80
31	Oak Creek at Sedona, AZ	9504430	603	657	19-Feb	14	586	12-Mar-82
32	Verde River near Paulden, AZ	9503700	5,569	657	20-Feb	32	445	20-Feb-80
33	Verde River near Clarkdale, AZ	9504000	8.130	1.507	20-Feb	35	1,433	21-Feb-80
34	Verde River near Camp Verde, AZ	9506000	12,028	3,370	20-Feb	18§	2,747	3-Mar-38
35	Gila River below Painted Rock Dam, AZ†	9519800	131,857	906	26-Feb	36	260	3-May-83
36	Gila River near Mohawk, AZ†	9520360	143,564	773	1-Mar	20	121	20-Apr-80
37	Gila River near Dome, AZ†	9520500	149,832	818	3-Mar	36	136	18-Sep-63

*Only stations with more than 10 years of record are shown. Data from Smith et al., 1994.
†Drainage regulated above station. Period of record corresponds to period of affected flow.
§Period of record is not continuous.

terns and antecedent seasonal precipitation conditions prior to and during the flood (*flood hydroclimatology*), and (3) the *physiography*, that is, the drainage basin characteristics of the stream systems that must accommodate the excessive runoff.

Flood hydrometeorology focuses on the sequence of local weather events occurring over minutes, hours, and days that are the most immediate—or proximate—causes of flooding. These short-term, local-scale meteorological events emerge from a longer-term (weeks, months, seasons, years) and larger-scale (regional, hemispheric, global) context that has been defined as "flood hydroclimatology" (Hirschboeck, 1988). Flood hydroclimatology places regional hydrometeorologic flooding activity in the context of its history of variation over a longer period of time that includes preceding weeks, months, seasons, and years. It also examines the uniqueness of flooding events in terms of their antecedent conditions and the spatial framework of the regional and global network of changing combinations of meteorological elements such as storm tracks, air masses, pressure-height anomalies, and other components of the large-scale circulation. Consideration of floods in their hydroclimatological context allows individual flood events to be linked to atmospheric phenomena operating at longer time scales and global spatial scales. Physiography is the terrestrial component of the three factors that generate floods. We use the term physiography to refer to all physical aspects of a drainage basin: topography (e.g., elevation distribution, relief, drainage density, basin shape), vegetation, land use, soil characteristics, and geology. These are the factors that influence the storage, distribution, and ultimate concentration of

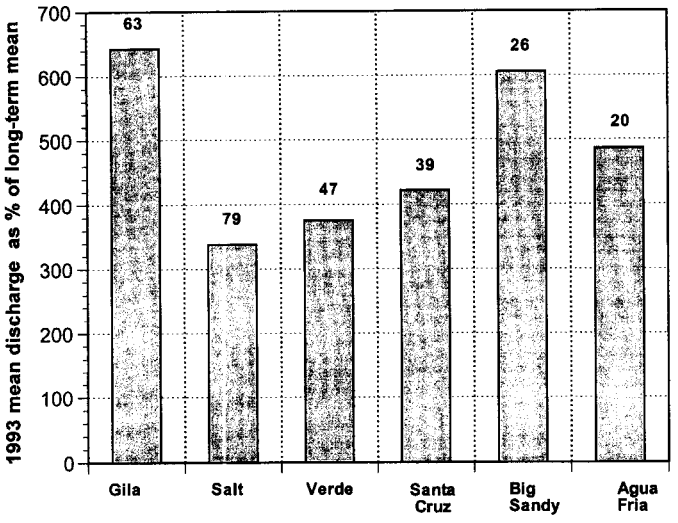

Figure 2. 1993 mean annual discharge expressed as a percentage of the long-term mean for selected, unregulated streams in Arizona. Numbers above the bars correspond to the length of record (years) on which the long-term mean is based. Data from Smith et al. (1994).

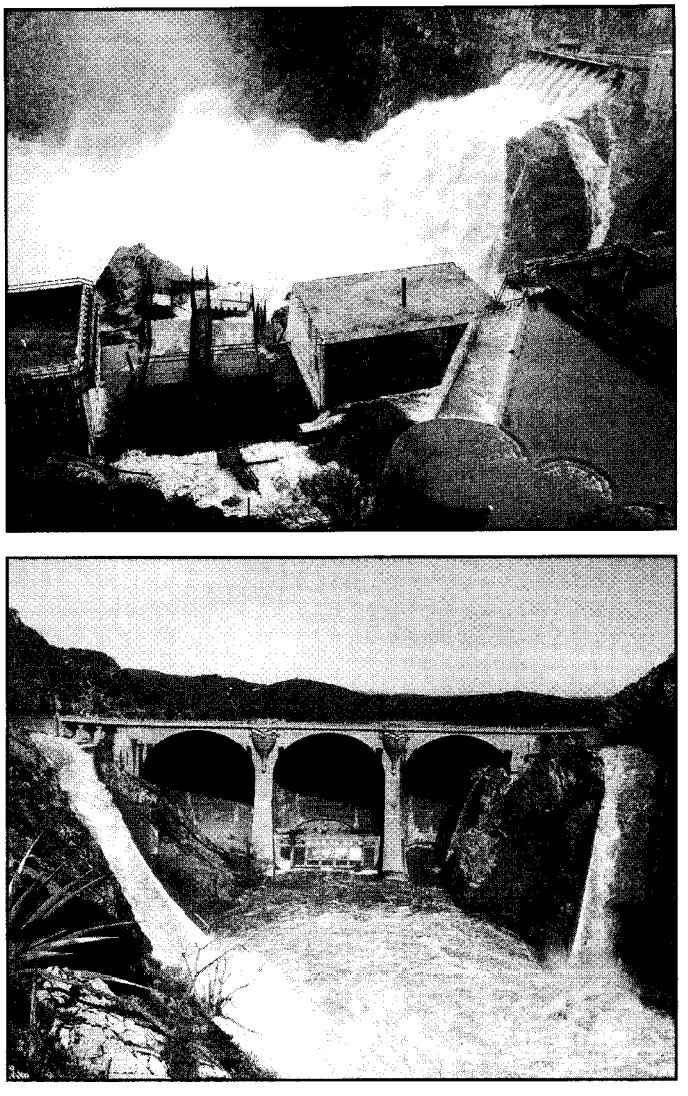

Figure 3. Photographs of two major dams in Arizona adversely affected by flooding during the winter of 1993. Upper photo, Roosevelt Dam on the Salt River, January 19, 1993. Lower photo, Coolidge Dam on the Gila River, January 16, 1993. Photographs provided by the U.S. Bureau of Reclamation.

atmospheric moisture into runoff. Basin physiography is the component that integrates precipitation from discrete weather events, which are embedded in the larger-scale circulation features, into flood peaks, flood volumes, and flow durations.

FLOODING IN ARIZONA—PHYSIOGRAPHY, CLIMATOLOGY, AND DRAINAGE

The physiography and climatology of Arizona provide the framework for a spatially and temporally diverse flooding regime. In order to place the Arizona floods of 1993 in context, first we will provide an overview of the physiographic and climatic setting in which the floods developed. In the following sections the discussions of the climatology of Arizona are derived from Sellers and Hill (1974), Hirschboeck (1985, 1987), Webb and Betancourt (1992), and Ely (1992).

Basin and Range Province

Arizona comprises three distinctive physiographic provinces: the Basin and Range, Colorado Plateau, and Central Highlands (Fig. 1). The western, south-central, and southeastern parts of Arizona make up the Basin and Range Province. It is characterized by widely spaced mountain ranges of relatively limited extent separated by wide, low-lying alluvial valleys. The highest mountains in the province are located in the southeastern portion where elevations in excess of 2,740 m (9,000 ft) are common. Maximum elevations rarely exceed 1,525 m (5,000 ft) in the western portion.

The climate of the Basin and Range Province varies from arid in the west to semiarid in the southeast. Rainfall in the region is characterized by a distinct bimodal seasonality with a precipitation maximum in summer and a secondary maximum in winter. Overall, rainfall totals are highest in the southeast because of a greater orographic influence than exists in the western portion. Most streams in the Basin and Range Province are ephemeral. Some streams with perennial reaches occur in the southeastern portion.

Summer precipitation and occasional flash flooding occur in the Basin and Range Province as a result of intense convectional thunderstorms during seasonal influxes of atmospheric moisture from the Pacific Ocean, the Gulf of California, or humid regions of tropical Mexico. In some years the summer precipitation season is enhanced or prolonged into fall by rainfall associated with excess moisture from tropical storms in the eastern North Pacific Ocean or Gulf of California. Winter precipitation is primarily associated with passing fronts. Some frontal storms are associated with warmer, subtropical atmospheric flow and yield only rainfall. Others are southerly displaced cold fronts that deliver rainfall to the valleys and snow to the upper elevations, except in the western portion where snowfall is rare. Winter snow accumu-

lation and subsequent melting are not major sources of flood runoff in the Basin and Range Province in Arizona except locally in the southeastern portion.

Central Highlands Province

The Central Highlands Province has very rugged topography characterized by closely spaced mountain ranges and deep canyons. Elevations range from around 305 m (1,000 ft) to about 2,740 m (9,000 ft) on the highest peaks. The orientation of the rugged Central Highlands Province is roughly northwest-southeast, thus presenting a prominent orographic barrier to storms coming in from the southwest across the low desert. The Central Highlands Province is separated from the considerably less rugged Colorado Plateau by the Mogollon Rim, which is a distinct erosional escarpment along most of its length. The southwest face of the rim is dissected by deeply incised canyons that flow through the Central Highlands toward the south and west.

Like the Basin and Range Province to the south, the precipitation regime in the Central Highlands Province has a distinct bimodal seasonality. However, larger winter precipitation totals (rain and snow) occur because of a higher frequency of winter frontal storm passages and a more pronounced orographic effect. Summer precipitation totals are also somewhat higher and result from more frequent, orographically enhanced, convective storm activity and occasional influxes of moisture from Pacific tropical storms.

Many streams draining the Central Highlands and Mogollon Rim maintain perennial flow as a result of a precipitation-enhancing orographic effect that activates summer convectional showers and fosters the accumulation of snow from winter frontal storms. In the larger drainage basins, substantial snow accumulations can have an important effect on winter and spring flooding. Snowmelt runoff and rain falling on snow are much more likely to generate flood runoff here than in the Basin and Range Province to the south.

Colorado Plateau Province

The Colorado Plateau Province is a relatively low-relief, sparsely vegetated, high-elevation part of north-northeastern Arizona, with widely spaced mesas, buttes, and small, isolated mountain ranges. It exhibits the same bimodal precipitation regime as the Central Highlands Province to the south but has lower overall precipitation totals, especially in winter. This difference is due to the lack of a significant orographic influence, the effect of downslope adiabatic drying, and a greater distance from oceanic moisture sources. Most streams in this northern part of the state flow in response to local convectional thunderstorms in summer and precipitation from frequent frontal storms in winter. Occasionally in summer and fall, tropical storms provide a source of excess atmospheric moisture even as far north as the Colorado Plateau.

Major drainages in Arizona

The two largest river basins in Arizona are the Gila River Basin and the Lower Colorado River Basin (above the confluence of the Colorado River and the Gila River in western Arizona). The Gila River Basin includes most streams in the Basin and Range Province and most streams in the Central Highlands Province that drain toward the south away from the Mogollon Rim. The Lower Colorado River Basin includes much of the Colorado Plateau Province and is dominated by the Colorado and Little Colorado Rivers. Other tributary source areas in the Lower Colorado River Basin include a lesser portion of the Central Highland Province and extensive desert areas in the western Basin and Range Province.

Within the Gila River Basin, the Santa Cruz and San Pedro Rivers are the major systems draining the southeastern Basin and Range Province. They flow northward from source regions in Mexico (San Pedro River) and along the Arizona-Mexico border (Santa Cruz River). Some of their tributaries originate in the high elevations of the southeastern mountain ranges, but most of the drainage area in the Santa Cruz and San Pedro River Basins is below 1,220 m (4,000 ft).

The northern half of the Gila River Basin is dominated by the Salt and Verde Rivers. The entire basin of the Salt River is in the Central Highlands region, and many of its tributaries originate on the southern face of the Mogollon Rim. The headwaters of the Verde River are on the Colorado Plateau, but the majority of the basin is also within the Central Highlands Province. Most of the Verde River's major tributaries flow in canyons that are deeply incised into the Mogollon Rim. Both the Salt and Verde River Basins have large portions of their drainage areas above 1,830 m (6,000 ft).

The lower reaches of the Salt and Verde Rivers are extensively regulated for flood control, irrigation, and municipal water supply (Fig. 1). The rivers join east of Phoenix, where the name Salt River is retained for the trunk stream. Just west of Phoenix, the Salt River joins the Gila River. The Gila is the master drainage, ultimately draining 148,864 km^2 (57,477 mi^2). This is more than 50% of the total area of Arizona. The lower Gila River is also extensively regulated. It traverses the southern half of Arizona in an east-west direction and joins the Colorado River at Yuma, Arizona.

Hydroclimatic flooding regimes of Arizona

The interaction between seasonal climate and physiography in different regions of Arizona results in interesting contrasts in the flooding regimes of the major drainages. Because of distinctive combinations of the climatic processes involved in the generation of floods in Arizona—that is, frontal rainfall, convectional thunderstorm rainfall, tropical storm rainfall, and snowmelt—flood records from most Arizona stream gauges can be decomposed into hydroclimatically defined mixed distributions (Hirschboeck, 1985, 1987). This is an effective method for exploring the underlying hydroclimatic causes for individual events in a gauged flood record and for better evaluating the kinds of hydroclimatic conditions that are likely to generate the most extreme events, such as the floods of 1993.

To illustrate this "flood hydroclimatology" approach, Figures 4a and 4b depict the hydroclimatically decomposed flood

records for the Santa Cruz River at Tucson (USGS gauge no. 09482500; Fig. 4a), a drainage basin representative of the southeastern Basin and Range Province, and the Verde River below Tangle Creek (USGS gauge no. 09508500; Fig. 4b), a basin located principally in the Central Highlands Province. The discharges are presented in the form of standardized dimensionless z scores for easier comparison (Hirschboeck, 1985, 1987). The complete histogram of all peaks-above-base during the period 1950 through 1985 is shown for each stream on the left of Figure 4, with the largest annual flood peaks distinguished from other peaks greater than the station's base discharge (partial duration peaks). To the right of each stream's complete histogram, the same peaks have been regrouped into separate subgroup histograms according to what type of climatic process generated each flood: tropical storm rainfall, convectional rainfall, or frontal precipitation (rain and/or snow). The 1993 peaks have been plotted for each stream for comparison with the 1950–1985 gauged record.

This methodology shows that summer flooding as a result of convectional rainfall is more frequent in the southeastern Basin and Range Province, whereas winter flooding as a result of frontal storms and snowmelt is more common in the Central Highlands Province. This variation comes from geographic and physiographic influences on the types and frequencies of synoptic meteorological events. Although winter frontal precipitation can occur throughout Arizona, the influence of fronts is greater in the Central Highlands Province than in the Basin and Range Province to the south. The Central Highlands lie closer to the typical winter storm tracks that steer fronts across the western United States. Thus, the latitude of the Central Highlands Province, coupled with its orographic effect, leads to a higher frequency of floods from winter frontal precipitation (rain and snow) than is observed in the Basin and Range Province to the south.

Winter frontal storms produce floods in streams throughout much of Arizona, but the relative magnitude and frequency of these events are influenced by basin-specific physiographic characteristics. For the two basins compared in Figure 4, the Verde Basin has a larger contributing drainage area than that of the Santa Cruz Basin: 14,227 km^2 (5,493 mi^2) versus 5,755 km^2 (2,222 mi^2). The Verde River's larger drainage area influences the number and size of front-generated floods, because as basin area increases, the importance of intense convectional showers as primary flood-producing events tends to decrease. The dominance of frontal flooding in the Verde Basin is also influenced by the percentage of the basin at high elevations, where snow accumulation and subsequent melting contribute to the runoff. Thirty percent of the Verde River's drainage area is above 1,830 m (6,000 ft), whereas only 1.8% of the Santa Cruz River's drainage area is above this elevation (Hirschboeck, 1985).

Decomposition of the flood series into hydroclimatic subgroups yields information about the causes of the largest peaks in a stream's gauge record (Fig. 4). For the Verde River, the largest floods in the extreme upper tail of the histogram distribution (including the 1993 floods) are associated with the Verde River's most common flood-generating climatic mechanism: frontal precipitation (Fig. 4b). In addition, tropical storm–related precipitation events, although rare, play a role in generating floods significantly greater than the mean. In the Santa Cruz Basin to the south, floods are most likely to be generated by summer convectional rainfall. In contrast to the Verde River, however, most of the floods in the extreme upper tail of the Santa Cruz River's flood histogram were not generated by its most common flood-generating climatic mechanism. Instead the largest discharges resulted either from tropical storm events, such as the peak of record in October 1983 (Roeske et al., 1989), or from winter frontal events such as the 1993 floods (Fig. 4a). Differences between the relative magnitudes of floods from these two storm types in the Santa Cruz and Verde River Basins probably reflect the greater likelihood of a larger snowmelt contribution to winter flooding in the Verde River Basin.

The extreme nature of the 1993 floods is underscored by evaluating them within the overall hydroclimatic context of flooding in Arizona. Hydroclimatic analysis of flood series for other Arizona streams indicates that winter frontal events are most likely to generate the largest floods in large basins of the Central Highlands Province of Arizona (Hirschboeck, 1985, 1987; Ely, 1992; Ely et al., 1994). The events of winter 1993 clearly support this. However, even in southern Arizona, which tends to be dominated by flooding from summer convectional thunderstorms or infrequent tropical storms, the 1993 winter floods were comparable to the largest floods on record.

THE 1993 ARIZONA FLOODS

The floods of January and February 1993 were the result of record precipitation from the passage of an unusually high number of winter storm fronts. These fronts moved across Arizona as part of an active storm track that was located anomalously far to the south. Frontal precipitation was frequent and heavy throughout the Central Highlands and southeastern Basin and Range Provinces from December 1992 through February 1993. Many meteorological stations in central Arizona recorded precipitation totals more than 400% of normal in January alone (MacNish et al., 1993); furthermore, it has been suggested that recurrence intervals for some of the highest precipitation totals in central Arizona during January and February 1993 were greater than 100 yr and may have been between 500 and 1,000 yr (Guttman et al., 1993). The extreme and prolonged precipitation resulted in a significant regional flooding episode in which record floods were recorded statewide (Fig. 1; Table 1). The flood source areas were limited primarily to the Central Highlands the southeastern Basin and Range, and a small portion of the Colorado Plateau, but the impact of flooding was far reaching because major drainages from these source areas traverse large portions of the state.

What combination of factors led to this major flooding event? How unusual was it within the context of the long-term climatic history and paleohydrology of flooding in Arizona? How likely is it for a similar event to occur in the future, given the uncertainty of either a naturally fluctuating or radically

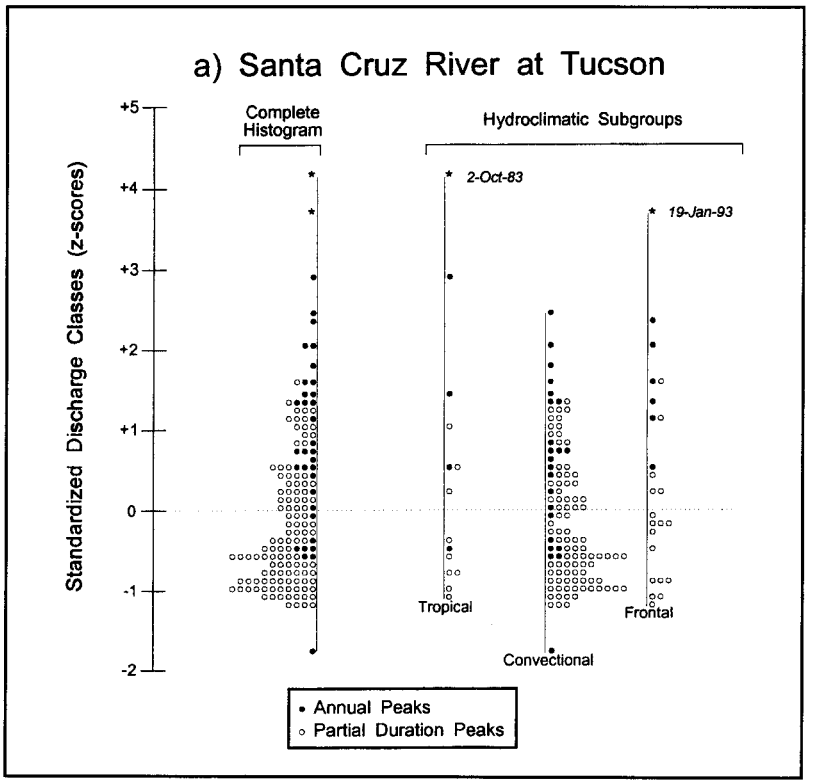

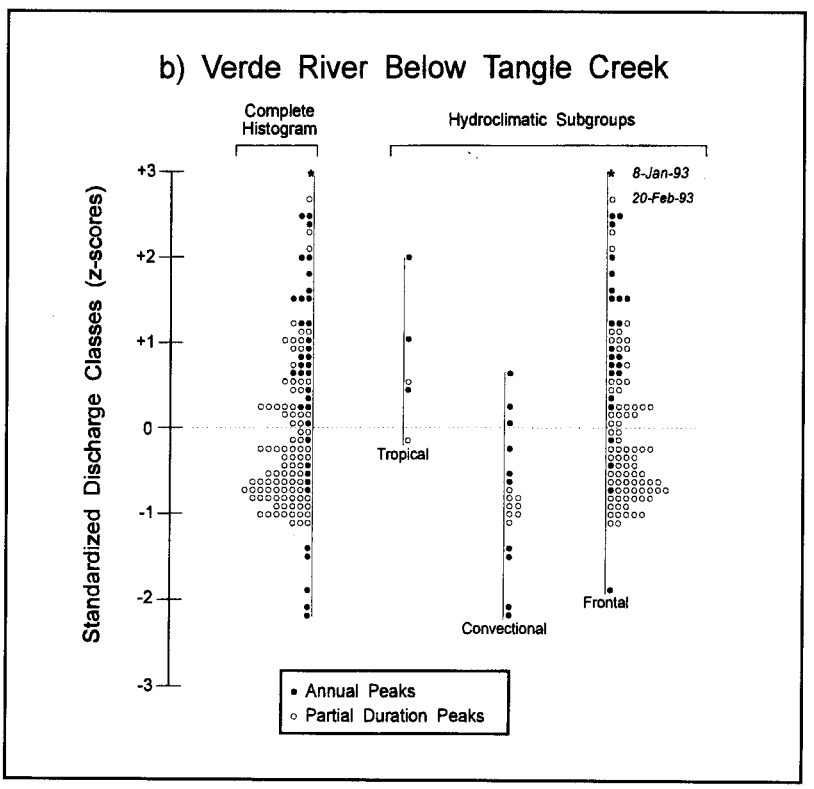

Figure 4. Decomposition of flood series from two gauging stations in Arizona according to hydroclimatic cause of flood. a, Santa Cruz River near Tucson; b, Verde River below Tangle Creek.

changing climate? We will examine these questions by presenting a detailed analysis of the hydroclimatic and physical aspects of the 1993 floods and then evaluating this information within the context of paleoflood evidence, regional historical peaks, and probable future climatic scenarios.

Atmospheric circulation features and related antecedent conditions

The hydrometeorological and hydroclimatological factors that led to the 1993 Arizona floods emerged from a series of global, hemispheric, and regional-scale climatic events. Global oceanic and atmospheric teleconnections related to El Niño–Southern Oscillation (ENSO) conditions influenced the development of large-scale atmospheric circulation anomalies in the eastern North Pacific Ocean. These anomalies were instrumental in developing flood-enhancing antecedent hydrologic conditions and in delivering precipitation that generated a sequence of large floods throughout the region.

El Niño–Southern Oscillation influences. An unusually strong, large-scale atmospheric circulation anomaly developed in the extratropical latitudes of the eastern Pacific Ocean and persisted in various forms throughout the winter of 1992–1993. During the previous winter of 1991–1992, El Niño conditions had persisted with above-normal sea-surface temperatures (SSTs) in the central and eastern tropical Pacific Ocean (Bell and Basist, 1994). By mid-1992 the index that characterizes the strength of the El Niño air-sea interaction had returned to normal, although SSTs remained above normal in the western tropical Pacific (Bell and Basist, 1994). During December 1992 and continuing through February 1993, above-normal SSTs again expanded eastward in the tropical and subtropical Pacific Ocean, and ENSO conditions redeveloped. Although not as strong as the previous winter's El Niño, winter 1992–1993 marked one of the longest periods of continuous warm SSTs on record for the tropical Pacific (Bell and Basist, 1994). The atmospheric circulation accompanying this SST anomaly was an enhanced subtropical jet stream that conveyed warm, moisture-laden air from the central equatorial Pacific to the southwestern United States.

Atmospheric circulation anomalies. Beginning in December 1992, an anomalous high-pressure area developed in the extratropical latitudes in the eastern North Pacific Ocean and persisted throughout the winter in varying degrees. This high-pressure blocking pattern over the Gulf of Alaska displaced one branch of the polar jet stream and associated Pacific storm track far to the north and another branch to the south. The southern branch combined with the enhanced subtropical jet stream. This split-flow configuration in the upper-level westerly flow led to above-normal extratropical cyclonic storm activity moving into the western United States unusually far to the south.

The anomalous and persistent atmospheric circulation patterns in January and February are depicted in Figures 5a and 5b. The broad, lightly shaded arrows indicate the mean trajectories of the two branches of the split westerly flow at the 500-mb pressure height (roughly 5 to 6 km [3 to 4 mi] above sea level). The unusual nature of the circulation pattern in each month is revealed by the standardized anomaly contours that show how much higher or lower than normal the 500-mb pressure heights were in each month. The anomaly maps illustrate the atmospheric flow into the western United States, counterclockwise around the eastern Pacific trough (low-pressure anomaly center) just west of California and clockwise around the blocking ridge (high-pressure anomaly center) in the Gulf of Alaska. Also shown are the amount and trajectory of anomalous moisture delivery into the southwestern United States (in grams of water vapor/kilograms air/second) at low levels (850-mb height; usually below 1 to 2 km [0.6 to 1.2 mi] above sea level). In both January and February, the low-level atmospheric flow that transported this excess moisture generally followed the anomalous steering currents associated with the deep trough at the 500-mb level. December's circulation displayed a tendency toward a split-flow pattern with an anomalous trough in the eastern North Pacific west of California and a blocking ridge in the vicinity of the Gulf of Alaska. Although in December the transport of moisture into the southwestern United States at low levels was not significantly above normal, the high frequency of frontal storms that traversed the southwest that month resulted in greater than normal precipitation amounts (Bell and Basist, 1994).

The persistence of this large-scale circulation anomaly throughout the winter and the frequent recurrence of the split westerly flow configuration had a direct effect on both the individual storms that delivered flood-producing precipitation to Arizona and the antecedent conditions that evolved over time within individual drainage basins. The net result was to make the basins more and more susceptible to flooding as the winter progressed. Depending on the configuration of the daily circulation, frontal passages during December 1992 through February 1993 were associated with either cold or warm storms. During cold fronts, precipitation at the higher elevations accumulated as snow, but when an intervening warm front passed through, the warmer temperatures would instigate snowmelt, and any precipitation associated with the frontal storm would accelerate the melting process as a result of rain falling on the snow. This process repeated itself several times over the three month period.

Antecedent conditions: The importance of rain on snow. The persistence of the circulation anomaly in the eastern North Pacific Ocean and its unusually placed storm track was the ultimate cause of the severity of the winter flooding in Arizona, primarily because of its influence on two key hydrologic factors related to antecedent conditions: (1) soil moisture storage capacity and (2) snowmelt, especially in the Central Highlands region. In the first case, the unusual circulation delivered a long succession of storms that led to progressive saturation of the drainage basins such that eventually soil moisture storage capacities were exceeded in all catchments. Precipitation delivered by storms later in the season therefore immediately generated surface runoff. In the second case, shifts in the trajectory of the storm track across Arizona and its southward displacement resulted in alter-

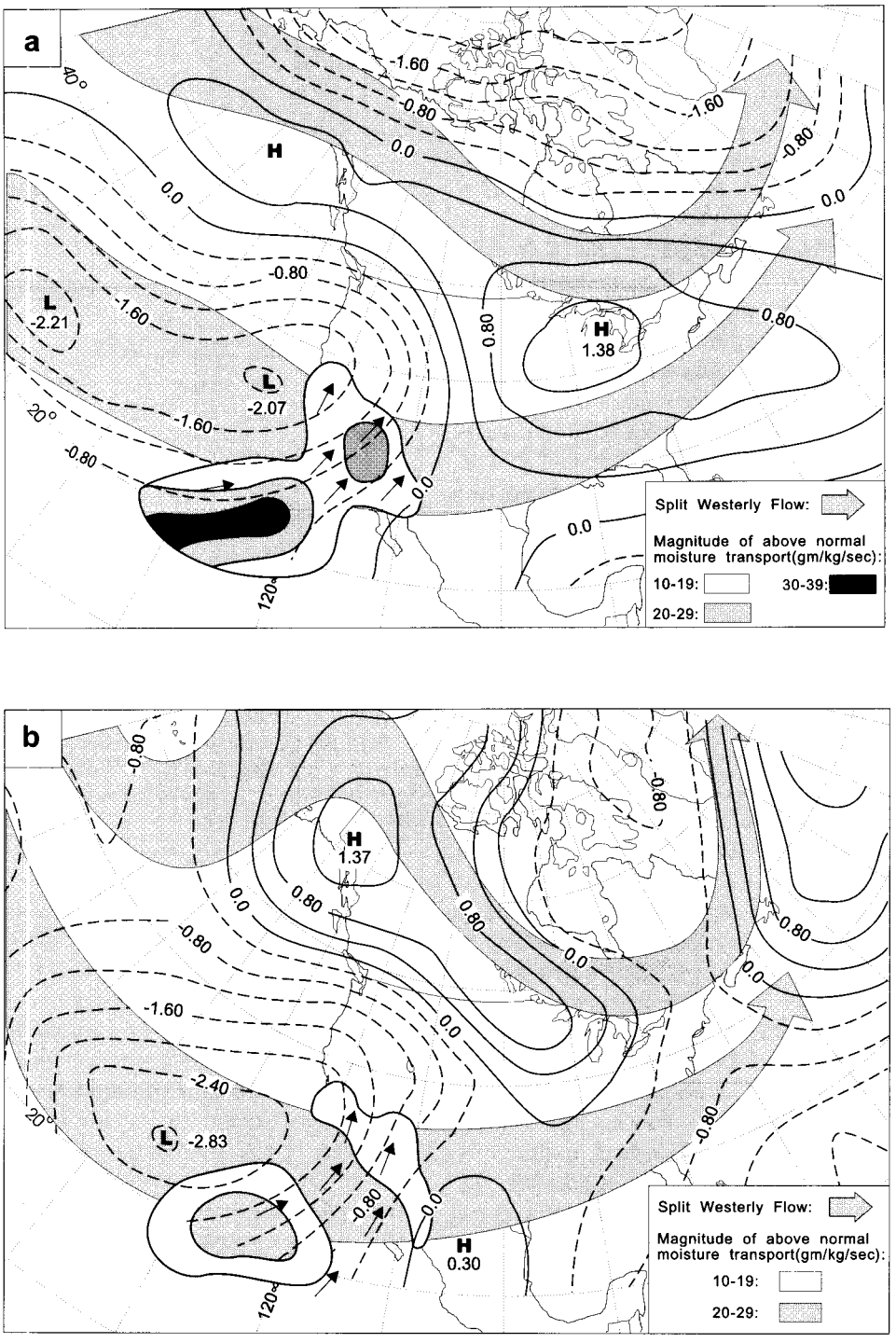

Figure 5. Anomalous upper-level atmospheric circulation and low-level moisture transport: a, January 1993; b, February, 1993. Circulation contour units are standardized anomalies (moisture information from Bell and Basist, 1994).

nating passages of warm and cold storms. This led to a complex sequence of events whereby snow accumulation and subsequent snowmelt, aided by rain falling on the snow, greatly augmented the amount of runoff.

Snowmelt caused by rain falling on snow was one of the most important hydroclimatic processes affecting the 1993 flooding. The temporal distribution of successive flood peaks during the course of the winter appeared to be a direct result of this phenomenon and its relation to the alternation of warm and cold storms. The relationship between rain-on-snow and runoff is illustrated in Figure 6. The daily variation in snowpack depth from December through February is shown, plotted with daily precipitation totals (rain and snow) for the Pinetop Fish Hatchery climate station in the Salt River Basin and the Flagstaff 4 SW climate station in the Verde River Basin (see Fig. 1 for approximate locations). These stations are representative of conditions throughout the high-elevation areas of the state where flooding was generated, particularly in the Salt and Verde River Basins.

The relationship between snow depth and precipitation at each station indicates the importance of both the occurrence and the timing of rain on snow in generating the largest floods. The antecedent conditions for flooding were initiated in early December when a cold front passage associated with a deep trough and upper-level cutoff low delivered large amounts of precipitation (rain at low elevations, snow at high) and a deep snowpack accumulated. Snow depths remained fairly constant throughout most of the month, with some minor variations in snowpack thickness occurring in response to winter cold front passages and intervening warming, respectively. However, during the last week of December 1992, a warm, subtropical storm moved into the state and dropped large quantities of rainfall. This subtropical event raised the snow level above about 2,590 m (8,500 ft; National Oceanic and Atmospheric Administration, 1992). Although depletion of the snowpack began during warming prior to the storm, the rain falling on the snow accelerated the depletion. However, as is evident in Figure 6, much of the snowmelt followed the rain event rather than coincided with it, especially at Flagstaff. Stream discharges rose in response to this event, but major flooding did not occur, probably because significant amounts of rain did not continue to fall during or after the period of most rapid snowmelt. Nonetheless, the December precipitation and snowmelt thoroughly saturated the soil in drainage basins at all elevations throughout much of Arizona. This had important consequences for establishing the antecedent conditions that intensified subsequent flooding (Fig. 6).

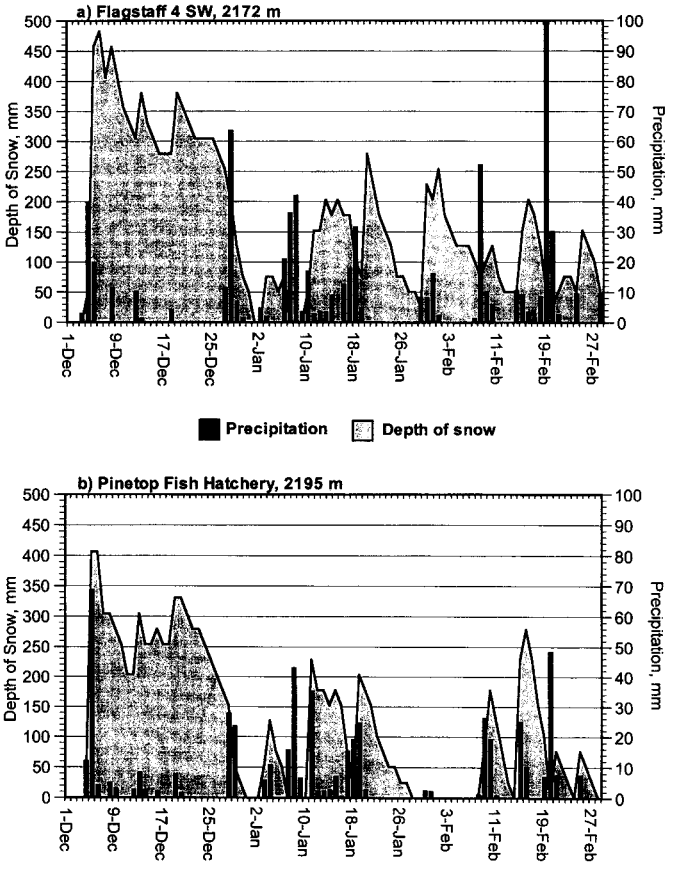

Figure 6. The relationship between precipitation and snow depth for two high-elevation stations in Arizona, December 1992 through February 1993: a, Flagstaff 4 SW; b, Pinetop Fish Hatchery. Precipitation shown corresponds to rain and snow. Data from National Oceanic and Atmospheric Administration (1992, 1993a, and 1993b).

The four major storms

The floods in Arizona were caused by at least 16 storms that passed over Arizona from December 1992 through February 1993 (House, 1993; NOAA, 1992, 1993a, 1993b). Most of the storms contributed to runoff and were important for developing and maintaining the antecedent conditions of soil saturation and accumulated snowpack necessary for the floods. However, four of the storms were the principal catalysts for the largest pulses of flooding that occurred during January and February. The number of individual storms that entered the region and the relative position of each storm track in relation to the position and characteristics of previous storms were reflected in the distribution of flood peaks throughout the state during this time period. Many streams had record or near record peaks in early January; others had record peaks in early February or late February. Some basins in the central portion of Arizona had large floods in response to each of the four major storm episodes that occurred. This rather complicated scenario is illustrated in Figure 7 with a series of normalized hydrographs for selected, unregulated basins in Arizona. Streams in the Central Highlands region best exhibited the four-peak flooding response.

The four major storms are defined for purposes of analysis as follows: (1) January 6–9, (2) January 13–19, (3) February 7–10, and (4) February 18–21. These time periods were chosen to best isolate the precipitation most directly associated with the major flooding episodes. We have, however, omitted some storms that were locally significant and regionally important in the development of antecedent conditions. Isohyetal maps for the four storm episodes are given in Figure 8, and composite 500-mb upper-air circulation maps for periods roughly coinciding with

these four storm periods are shown in Figure 9. The upper-air circulation maps show that a split westerly flow played a role during each of the four storm episodes. During the two main January storms (Figs. 8a-b, 9a-b), a persistent upper-air high pressure ridge in the Gulf of Alaska region was coupled with an equally persistent upper-air low pressure trough immediately to the south. This configuration displaced the southern branch of the North Pacific storm track to lower-than-normal latitudes so that storms and above-normal moisture were transported directly across Arizona (Fig. 5a). The two February storms (Figs. 8c-d, 9c-d) were also guided by an upper-air ridge-and-trough pattern. During these episodes, the Gulf of Alaska pressure ridge took the form of an omega-shaped blocking high pattern, and the attendant low pressure trough intruded deeply into subtropical latitudes, conveying warm, moisture-laden air into the southwestern United States from a more southerly trajectory. This was followed by the passage of a cold front as the trough moved through.

January 6–9. Following the precipitation that fell in December (particularly in the last week), the first major storm in January was the most widespread of the four flood-producing storm events (Fig. 8a). It followed a brief period during which temperatures dropped, precipitation fell, the freezing level dropped to 1,525 m (5,000 ft), and more snow accumulated at high elevations. On January 6, however, the snow level retreated to higher than 2,900 m (9,500 ft) when precipitation began to fall during the passage of a warm front. The warm front was associated with a disturbance of predominantly subtropical origin that was steered into Arizona by the southern branch of the split westerly flow. This system continued to deliver large quantities of rain for three days, with maximum amounts recorded on January 7. The timing of snowmelt and precipitation was optimal for flooding. This storm event virtually eliminated the snowpack in high-elevation parts of most drainage basins because of rain falling on the snow and relatively mild temperatures associated with the storm. More important, considerable rain continued to fall after the snowpack melted. This combination of events, coupled with the melt event at the end of December, culminated in the most regionally significant period of

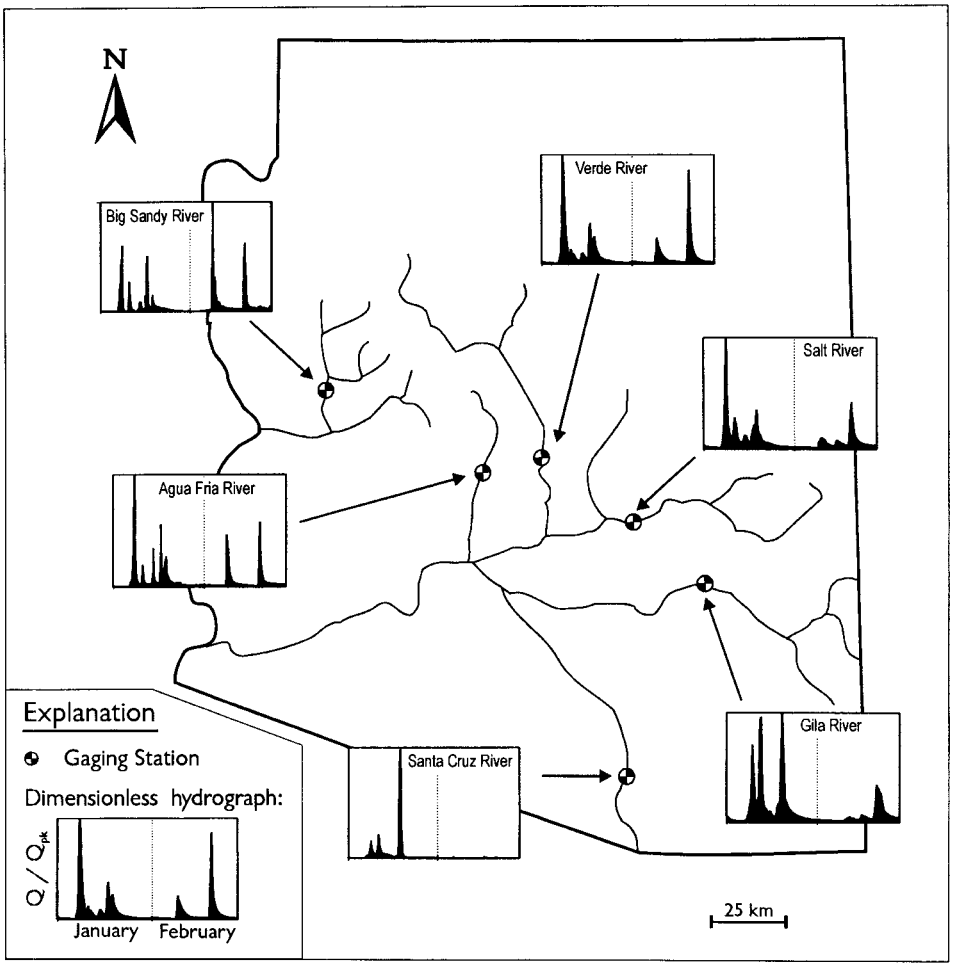

Figure 7. Map showing the spatial and temporal distribution and relative magnitude of flood peaks at selected (unregulated) basins in Arizona, January through February 1993. The vertical axis shows the ratio of hourly discharge to the maximum discharge in the two-month period. Based on data in Smith et al., (1994) and provisional data from the U.S. Geological Survey.

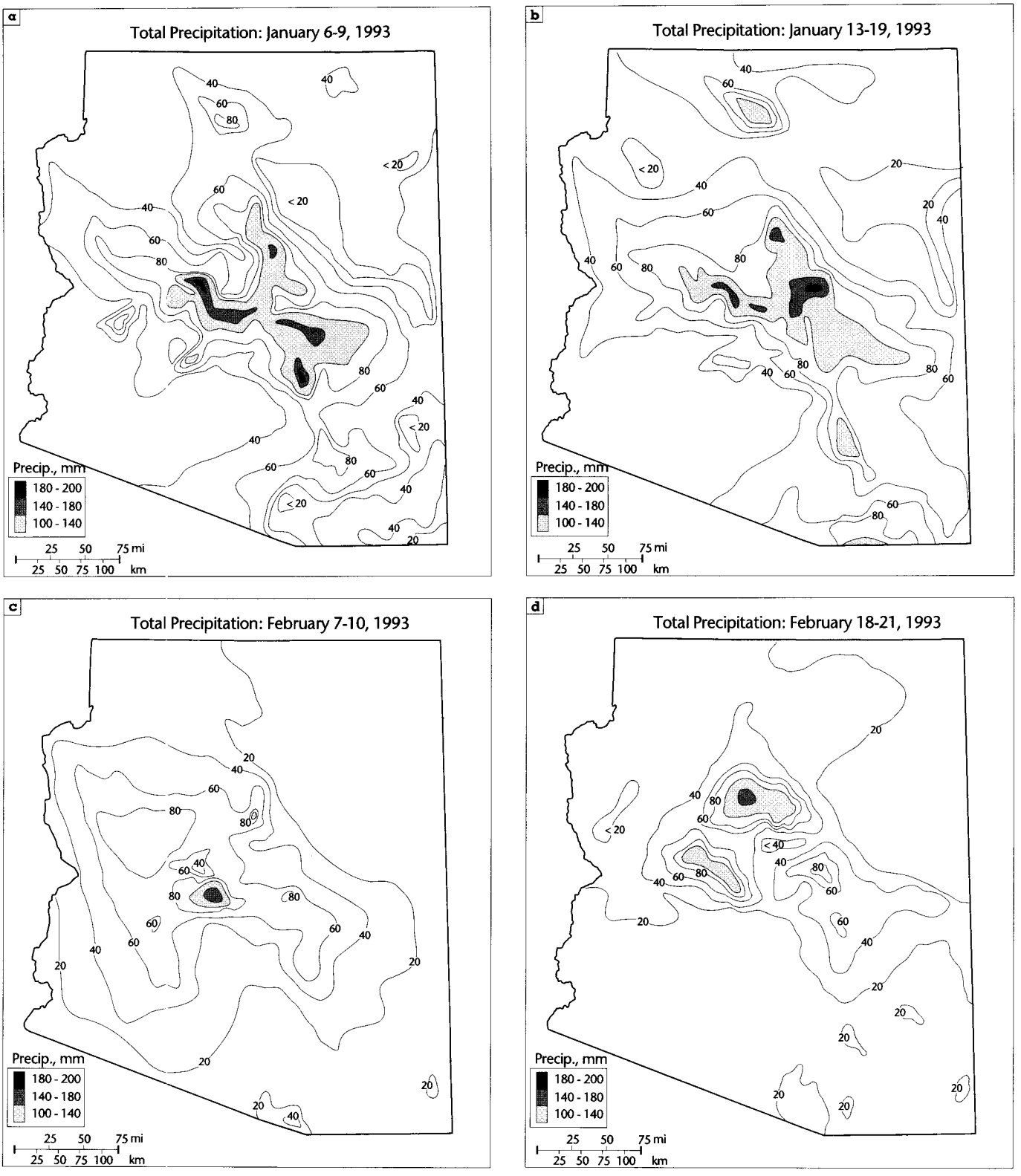

Figure 8. Isohyetal maps for the four periods of major regional flooding in Arizona, January through February 1993. a, January 6–9; b, January 13–19; c, February 7–10; d, February 18–21. Isohyets based on data from National Oceanic and Atmospheric Administration (1993a, 1993b) and unpublished data provided by the Maricopa County Flood Control District and the Salt River Project. Depths in mm. Depths in excess of 100 mm are indicated by shading.

flooding in the entire two-month episode and arguably the largest such episode since at least 1891. Most of the record peaks established in Arizona resulted from this storm (Table 1). Rainfall was particularly intense in the Central Highlands and in the higher ranges of the southeastern Basin and Range (Fig. 8a). Very large basins draining the Central Highlands (Salt and Verde Basins) had exceptionally large floods. Interestingly, flooding on the Santa Cruz River in the southeast was not as severe although several of its tributaries had record or near-record floods (Table 1; Fig. 7; Smith et al., 1994).

January 13–19. The widespread and heavy precipitation of the January 6–9 storm was followed by a similar, but less extreme, flood-producing event in the third week of January. This event culminated in flooding on January 19. During the January 13–19 period several fronts passed through Arizona steered along by the southern branch of the split westerly flow. The rainfall associated with these storms was heavy in the southernmost part of Arizona as well as in portions of the Central Highlands (Fig. 8b). Major flooding occurred along the Santa Cruz River during this episode, and the Gila River received a second pulse of peak flow only days after the first flood crest had attenuated (Fig. 7). At Flagstaff, the relationship between precipitation and snowmelt was less optimal for flooding than that of the early January event (Fig. 6). The snowpack was not depleted, and, in fact, it began to increase near the end of the storm period. Rainfall did not occur during the subsequent snowmelt. At Pinetop, conditions were slightly more favorable for flooding because more snow melt occurred during the initial rainfall. However, by the end of the episode, snow was accumulating there as well.

February 7–10. A shift in the configuration of the large-scale atmospheric circulation preceded the first major storm episode in February. The high-pressure ridge in the Gulf of Alaska shifted slightly to the east and increased in amplitude, bringing the axis of the ridge over western Canada (Fig. 9c). This change was associated with a southward movement of the eastern North Pacific trough and an increase in north-or-south directed flow (meridionality) in the circulation. The result was the continued conveyance of subtropical flow and moisture into the southwest (Fig. 5b) that was directed northward into Arizona behind a warm front. This was rapidly followed by a cold front moving in from the west as the trough passed through. This synoptic situation was especially effective in delivering large amounts of precipitation to western, northwestern, and central parts of Arizona (Fig. 8c). Rivers in these areas, such as the Big Sandy and Agua Fria Rivers, experienced a third large flood during this episode. The Big Sandy River and two of its gauged tributaries recorded peaks of record (Fig. 7; Table 1). This flooding was probably a result of relatively localized, moderate to heavy precipitation on saturated ground with some augmentation by snowmelt. During the cold-front passage that marked the end of this event, some precipitation was delivered in the form of snow, as seen at Flagstaff and Pinetop where snow levels decreased to 2,135 m (7,000 ft) and snowpack depths increased (Fig. 6).

February 18–21. As late February approached, the blocking high-pressure anomaly returned to its earlier position over the Gulf of Alaska, maintaining a split flow in the westerlies and a trough displaced to lower latitudes of the eastern North Pacific (Fig. 9d). Warming occurred in Arizona as a result of the southwesterly flow under this configuration. On February 17, relatively rapid melting of the accumulated snowpack occurred as a result of a regional increase in average daily temperature (near 10 °C [50 °F] at Flagstaff). Beginning late on February 18, this melting episode was dramatically punctuated by precipitation from the last major storm of the season (Fig. 8d). The rapid passage of two fronts in a two-day period produced heavy precipitation over localized areas in the Central Highlands and, in particular, over the central Mogollon Rim in the general vicinity of Flagstaff. This area received extremely high daily totals of precipitation on February 19 and 20. The heavy rain fell on the melting snowpack and resulted in the rapid generation of immense quantities of runoff. Large floods occurred on several streams draining these localized areas (Figs. 10 and 11; Tables 1 and 2). The runoff was concentrated in a small part of the Verde River basin, but it was sufficient to generate the flood of record at the Verde River gauging stations at Paulden, Clarkdale, and Camp Verde (Table 1; Fig. 1). It also amounted to the second-largest flood ever recorded at the gauge below Tangle Creek. A flood of this magnitude coming from such a small part of the basin is evidence of the optimum, flood-enhancing antecedent conditions that existed at the time, and thus, the importance of preceding events in December, January, and most of February.

Rain falling on snow was a very important factor in the generation of the largest 1993 floods, especially in the large basins of the Central Highlands. The strong correspondence between streamflow, snowmelt, and precipitation in the winter of 1992–1993 is shown in Figure 10, where daily values of snowmelt and precipitation at Flagstaff are plotted with the average daily discharge of Oak Creek near Cornville, Arizona. This figure illustrates the sensitivity of stream flow to the timing and relative magnitude of the rainfall in relation to the snowmelt. It suggests that the largest flood peaks will occur when rain falls on snow, accelerating the melting process, and then continues to fall.

THE 1993 FLOODS IN THE VERDE RIVER BASIN

The remaining discussion of the 1993 winter flooding episode in Arizona will focus on flooding in the Verde River Basin during January and February. The Verde River Basin provides an excellent and detailed perspective on many of the important characteristics of the flood episode. Extreme, record-breaking discharges were recorded at all gauges along the Verde River and on most of its principal tributaries during January and February 1993 (Fig. 11). Because of the size, spatial distribution, and diverse physiography of the Verde River Basin, flooding in different portions of the basin exhibited important aspects of the spatial and temporal variation that characterized the flooding throughout Arizona. Additionally, post-1993 flood studies and past research on the paleoflood history of the Verde River allow us to make gener-

alizations about the relative magnitude of the 1993 floods with respect to the largest floods known to have occurred over the last 1,000+ yr (House, 1996; House et al., 1995).

Gauging records from the Verde River Basin

The Verde River Basin spans nearly 15,000 km^2 (5,800 mi^2) of central Arizona. Its headwaters and the headwaters of many of its tributaries encompass a large portion of the Colorado Plateau, but the Central Highlands constitute the bulk of the flood-producing portion of the basin. Four continuous recording gauges are located along the Verde River (Fig. 11). The uppermost gauge is near Paulden, Arizona (USGS gauge no. 09503700). Its contributing drainage area is 5,569 km^2 (2,150 mi^2), which is about 40% of the total basin area. It records runoff draining the Colorado

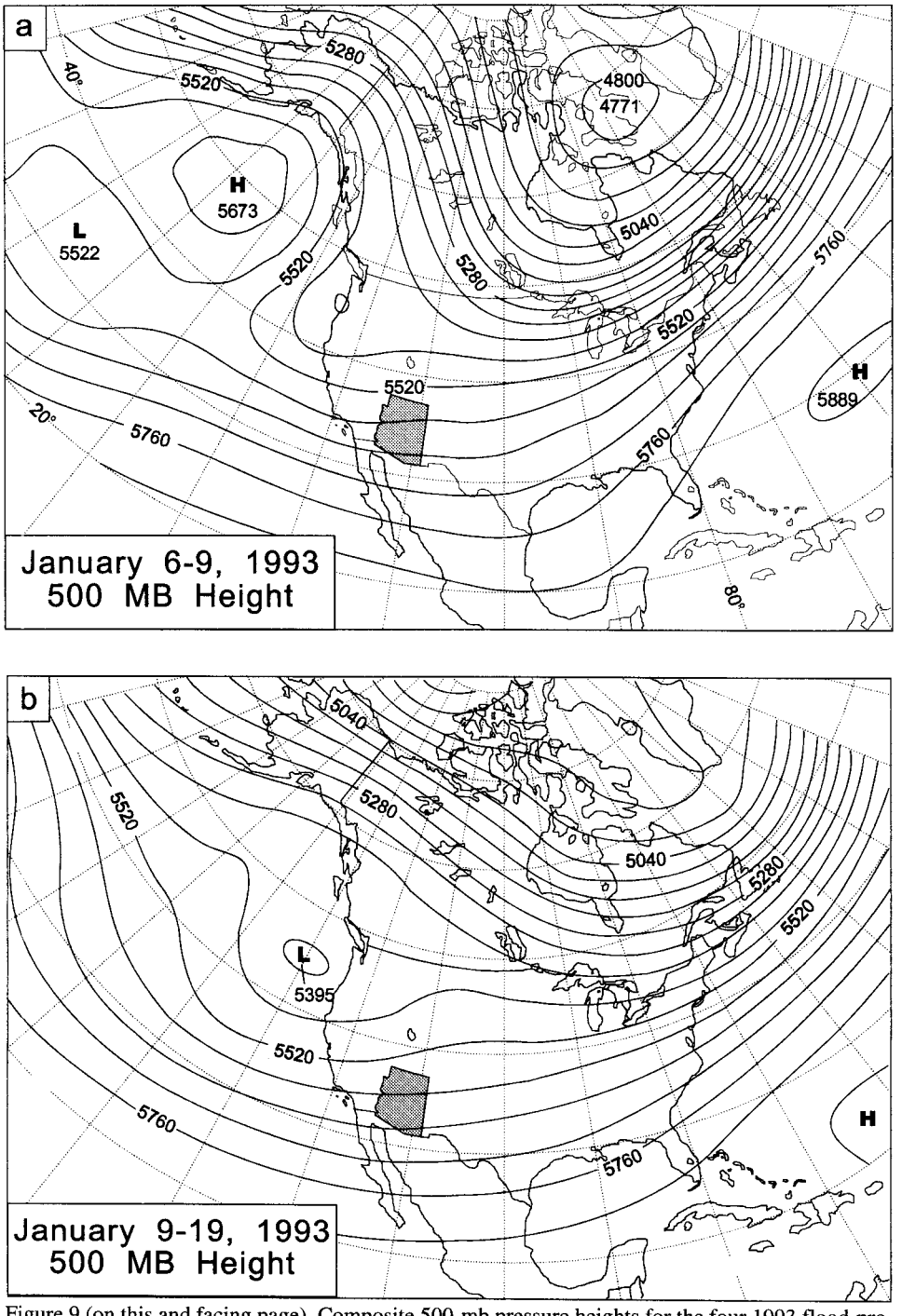

Figure 9 (on this and facing page). Composite 500-mb pressure heights for the four 1993 flood-producing storm episodes. Units are geopotential height in meters above sea level. a, January 6–9; b, January 9–19; c, February 8–10; d, February 19–20.

Plateau and a northeast-facing part of the Central Highlands region. Despite the size of this portion of the Verde Basin, little contribution from it is recorded in the peak discharges at gauges downstream because flood peaks at Paulden usually follow, rather than precede, those at the next gauge downstream by several hours. This lag is probably a result of the relatively elongated shape of the upper basin, circuitous drainage routes, and minor storage effects of Sullivan Lake, just upstream of the gauge (Chin et al., 1991).

Downstream from Paulden, the next gauge is near Clarkdale, Arizona (USGS gauge no. 09504000). Its contributing drainage area is 8,130 km^2 (3,146 mi^2) which accounts for about 60% of the total basin area or 30% of effective flood peak-producing area (i.e., the area below the gauge at Paulden). About 75% of the area between Paulden and Clarkdale is drained by Sycamore and Hell Canyons. Sycamore Canyon is one of the largest single tributaries in the Verde River system. It enters the Verde River from the north, approximately 2.6 km (1 mi) above the gauge. During the 1993 events, Sycamore and Hell Canyons probably accounted for much more than 50% of the runoff at the Clarkdale gauge. Unfortunately, neither one of these tributaries is gauged.

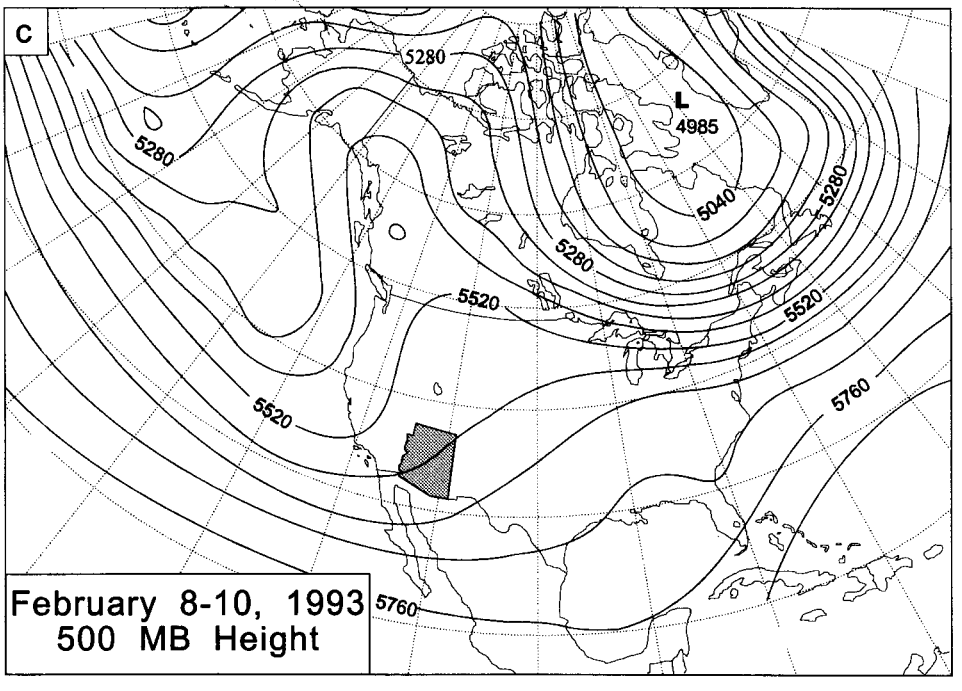

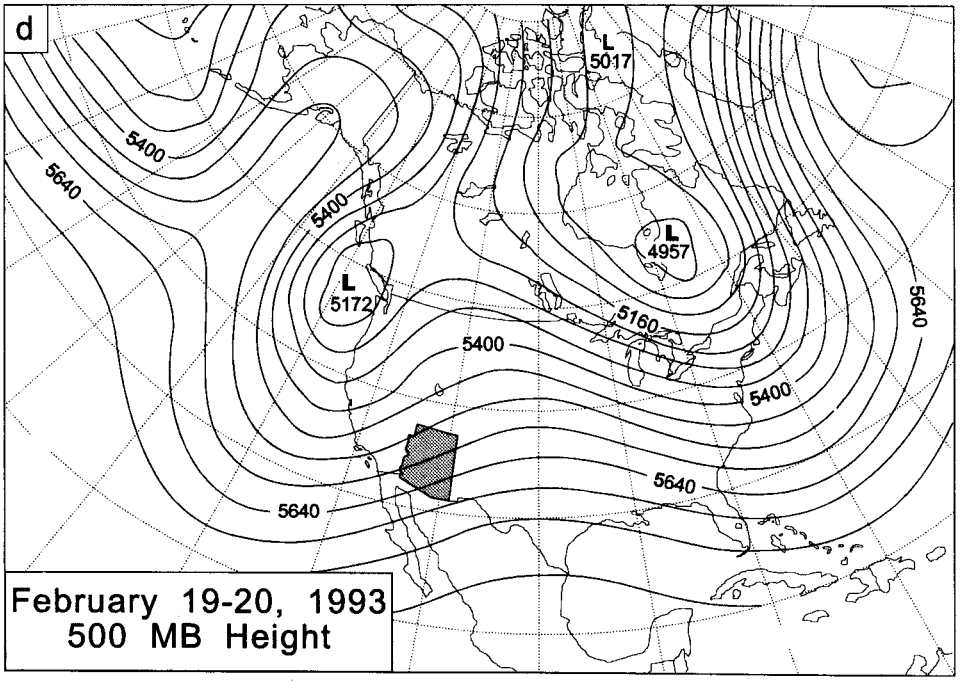

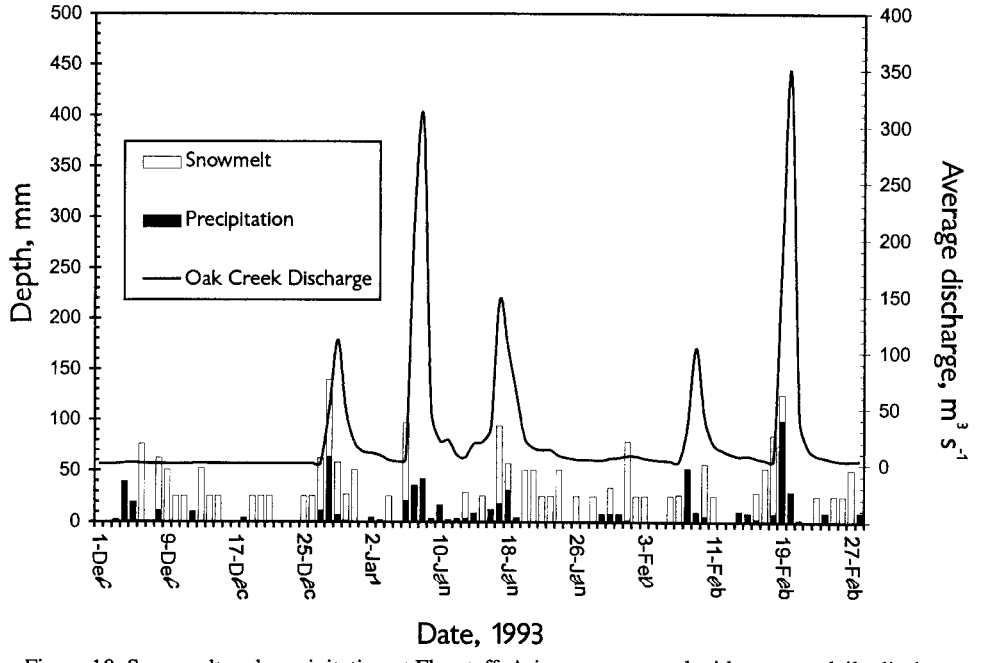

Figure 10. Snowmelt and precipitation at Flagstaff, Arizona, compared with average daily discharge of Oak Creek near Cornville, Arizona (USGS gauge no. 09504400). As shown, snowmelt is the change in the depth of the snowpack and not the actual water content of the melt. Data from National Oceanic and Atmospheric Administration (1992, 1993a, 1993b), Smith et al., (1994), and provisional data from the U.S. Geological Survey.

The gauge below Clarkdale is near Camp Verde, Arizona (USGS gauge no. 09506000). Its contributing drainage area is 12,028 km^2 (4,652 mi^2), which is 85% of total basin area or 75% of the effective area. Between Clarkdale and Camp Verde, four relatively large, gauged tributaries enter the Verde River: Oak Creek (920 km^2, 355 mi^2; USGS gauge no. 09504500), Dry Beaver Creek (368 km^2, 142 mi^2; USGS gauge no. 09505350), Wet Beaver Creek (288 km^2, 111 mi^2; USGS gauge no. 09505200), and West Clear Creek (624 km^2, 241 mi^2; USGS gauge no. 09505800) These gauge sites are shown on Figure 11. The four tributaries account for about 55% of the drainage area between the mainstem gauges of Clarkdale and Camp Verde. Each tributary drains high-elevation terrain on the Colorado Plateau above the southwest face of the Mogollon Rim. Other small, ungauged tributaries from the northeastern side of the Central Highlands also enter the river between the gauges, but their relative contribution is small in relation to the Rim tributaries. The final gauge on the unregulated portion of the Verde River is located below Tangle Creek (USGS gauge no. 09508500). It records runoff from a total of 15,170 km^2 (5,857 mi^2), including an additional 2,200 km^2 (850 mi^2) below the Camp Verde gauge. The majority of this area is within the rugged interior of the Central Highlands. The difference in the hydrographs between Camp Verde and Tangle Creek primarily represents differences in the relative amounts of runoff contributed by the Mogollon Rim and interior Central Highland portions of the basin. Two gauged tributaries enter in this reach: the East Verde River (857 km^2; 331 mi^2; USGS gauge no. 09507980) and Wet Bottom Creek (94 km^2; 36.4 mi^2; USGS gauge no. 09508300). Many ungauged tributaries also enter in this part of the basin, and they can account for large contributions of runoff.

Flood hydrographs in the Verde River Basin: January and February 1993

The map of the Verde River Basin in Figure 11 shows normalized hydrographs for each gauging station within the basin. The hydrographs exhibit variable responses to the two-month series of storms, and the basinwide pattern is very similar to the statewide pattern depicted in Figure 7. Each of the basins was affected by each flood-producing storm to some degree, and some basins responded to almost every precipitation event in the two-month period. The most pronounced characteristic of the basinwide response was the relative difference between the early January and late February peak discharges within different parts of the basin. The normalized hydrographs indicate that most of the gauges, with the exception of the Verde River at Paulden and Clarkdale, recorded relatively large floods in early January; however, for most sites in the middle and upper parts, the peak in late February was the largest. The early January and late February peak discharges at the Tangle Creek gauge constituted the largest and second-largest peaks recorded at this site, respectively. Their extreme magnitudes were reflected in a massive accumulation of flood debris in a broad alcove less than 1 km (~0.5 mi) above the gauge (Fig. 12). A comparison of the flood hydrographs at different gauges along the main stem of the Verde River (Fig. 13) suggests that different source areas contributed to the peak discharge recorded at the Tangle Creek

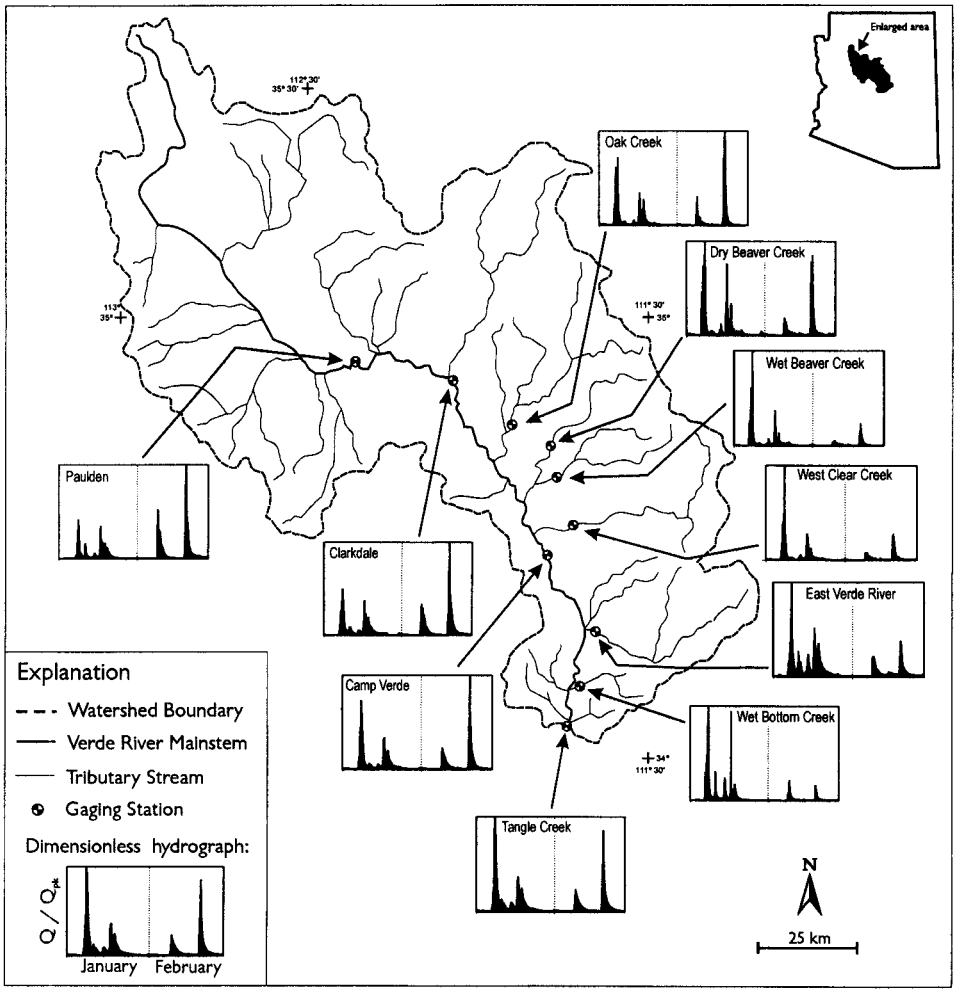

Figure 11. Spatial and temporal distribution and relative magnitude of flood peaks at all gauging stations in the Verde River Basin, January through February 1993. Vertical axis shows the ratio of the hourly discharge to the maximum discharge recorded in the two-month period. Based on data in Smith et al., (1994) and provisional data from the U.S. Geological Survey.

gauge during both major floods. Examination of hydrograph and precipitation data indicates that the relatively small area between Camp Verde and Tangle Creek may have contributed more than 65% of the early January peak. In contrast, during the late February flood, a small part of the basin between Paulden and Camp Verde contributed more than 95% of the peak recorded at Tangle Creek (House, 1996; House et al., 1995).

The early January event. The early January event is the largest recorded discharge at the gauge below Tangle Creek and the third-largest discharge recorded at the gauge near Camp Verde. The discharges were 4,106 $m^3\ s^{-1}$ (145,000 $ft^3\ s^{-1}$) and 2,478 $m^3\ s^{-1}$ (87,500 $ft^3\ s^{-1}$), respectively. At the Tangle Creek site, the only officially recognized flood larger than 1993 was the flood of February 1891, which is reported as 4,248 $m^3\ s^{-1}$ (150,000 $ft^3\ s^{-1}$; Patterson and Somers, 1966).

The occurrence of peak discharge at the Paulden, Clarkdale, and Camp Verde gauges followed the peak at the downstream Tangle Creek gauge by varying amounts. Because the peak at the Camp Verde gauge followed the peak at the Tangle Creek gauge by four hours, we can assume that only a portion of the rising limb of the Camp Verde hydrograph contributed directly to the peak recorded downstream (Fig. 13a; Table 2). This suggests that an immense amount of runoff from the interior Central Highlands had to have been introduced to the river between the two stations—on the order of 2,690 $m^3\ s^{-1}$ (95,000 $ft^3\ s^{-1}$). The occurrence of maximum discharge later in the afternoon at the gauge near Camp Verde and at most of the middle- and upper-basin tributary gauges contributed significantly to the sustained high flow and enormous volume recorded at the Tangle Creek gauge, where the discharge exceeded 3,960 $m^3\ s^{-1}$ (140,000 $ft^3\ s^{-1}$) for more than four hours and exceeded 3,400 $m^3\ s^{-1}$ (120,000 $ft^3\ s^{-1}$) for more than 10 hours.

The unusual timing of the early January peaks recorded at the Camp Verde and Tangle Creek gauges arose from a chance

TABLE 2. THE MAGNITUDE AND TIMING OF PEAK DISCHARGES IN THE VERDE RIVER BASIN, JANUARY AND FEBRUARY 1993*

Station	Area	Flood of Jan. 8		Flood of Feb. 20	
		Time	Peak Discharge	Time	Peak Discharge
	(km^2)		(m^3s^{-1})		(m^3s^{-1})
Verde River near Paulden	5,569	19:30	257	9:45	657
Verde River near Clarkdale	8,130	13:00	745	4:00	1,507
Oak Creek near Comville	919	11:45	524	3:30	736
Dry Beaver Creek near Rimrock	368	9:15	329	5:15	280
Wet Beaver Creek near Rimrock	287	6:30	453	1:30	107
West Clear Creek near Camp Verde	624	8:00	702	1:00	195
Verde River near Camp Verde	12,028	13:00	2,478	11:00	3,370
East Verde River near Childs	857	8:00†	569	2:45	217
Wet Bottom Creek near Childs	94	7:00	209	0:00	34
Verde River below Tangle Creek	14,227	8:30	4,106	16:00	3,512

*Data from Smith et al., 1994.
†Estimated.

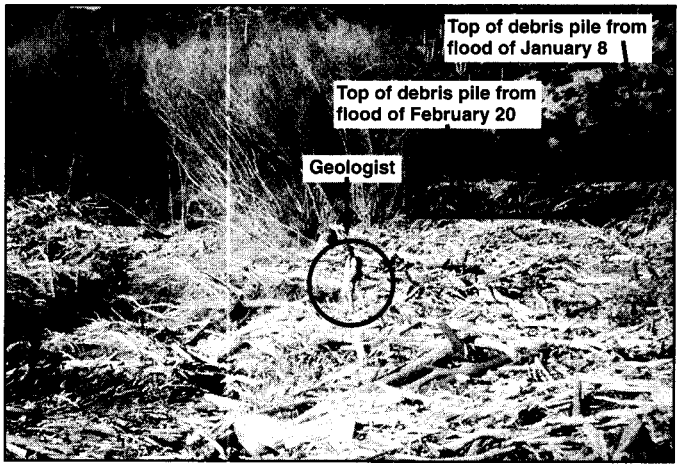

Figure 12. Large debris pile on lower Verde River, March 10, 1993. Photograph by P. A. Pearthree, Arizona Geological Survey.

combination of hydrologic events in the middle basin (the area between the Paulden and Camp Verde gauges) and the lower basin (the area between the Camp Verde and Tangle Creek gauges). Tributary hydrographs indicate that two distinct pulses of peak runoff characterized the early January event (Fig. 14). These pulses of runoff corresponded to similar variations in rainfall recorded in the middle and lower portions of the Verde River Basin. The second peak in the flood hydrographs is greater than the first peak in both portions of the basin, but their relative difference is greater in the lower basin than in the middle basin. From this relation we conclude that the exceptionally large peak recorded at the Tangle Creek gauge at 8:30 A.M., January 8, resulted from the coincidental, nearly optimal combination of the first peak from the middle basin with the second peak from the lower basin. The subsequent peak recorded at Camp Verde of 2,475 $m^3 s^{-1}$ (87,500 $ft^3 s^{-1}$) at 1:00 P.M., January 8, contributed to the sustained high flow recorded at Tangle Creek for most of the day. This situation illustrates the possibility that considerably different flood magnitudes could have occurred at the Camp Verde and Tangle Creek gauges given slight variations in the timing of rainfall and runoff in different portions of the basin.

The late February event. The late February event exceeded the magnitude of the early January flood at most of the gauging stations in the upper and middle portion of the basin. The limited spatial extent of this storm is evident in the distribution of flood peaks and can be inferred from the precipitation distribution in Figure 8d. The sharp precipitation gradient is reflected in the strikingly different relative magnitudes of the floods at Wet and Dry Beaver Creeks: two basins along the Mogollon Rim that are relatively close together (Fig. 11). At the Tangle Creek gauge, the flood of February 19, 1993, was 3,510 $m^3 s^{-1}$ (124,000 $ft^3 s^{-1}$), which is the second-largest peak recorded at this site. At the gauge near Camp Verde, the peak discharge was 3,370 $m^3 s^{-1}$ (119,000 $ft^3 s^{-1}$), which is the largest discharge recorded there. In striking contrast to the early January flood, examination of hydrological and meteorological data suggests that the vast majority of the peak and volume of the late February flood came from only a small part of the basin between Paulden and Camp Verde (Fig. 13b). Most of the runoff in the late February flood came from Oak Creek, Dry Beaver Creek, and probably Sycamore and Hell Canyons. The runoff was relatively flashy as compared with the early January event, and the corresponding total flow volume was considerably less at each gauge site (e.g., less than about 50% of the total volume of the January flood at Tangle Creek).

Gauge records from late February clearly indicate the importance of runoff contributions from Oak and Dry Beaver Creeks; however, the critical roles of Sycamore and Hell Canyons can only be inferred by comparing the Paulden and Clarkdale hydrographs. Figure 13 and Table 2 show that there is a significant lag in the timing of the peaks at Paulden and Clarkdale, with the Paulden gauge recording a peak after the Clarkdale gauge in both the January and February events. This indicates that little of the runoff at the Paulden gauge was a source for the peak discharge at Clarkdale in either event. In the largest flood in late February, the discharge increased from less than about 113 to 1,510 $m^3 s^{-1}$ (4,000 to 53,200 $ft^3 s^{-1}$) between the gauges at Paulden and Clarkdale. It is likely that much of this runoff came from Sycamore and Hell Canyons, which make up almost 75% of the area between the gauges. Meteorological data from Flagstaff and Williams, Arizona, near the upper watershed of Sycamore Canyon, show that the rainfall and flooding conditions in the basin may have been equal to or

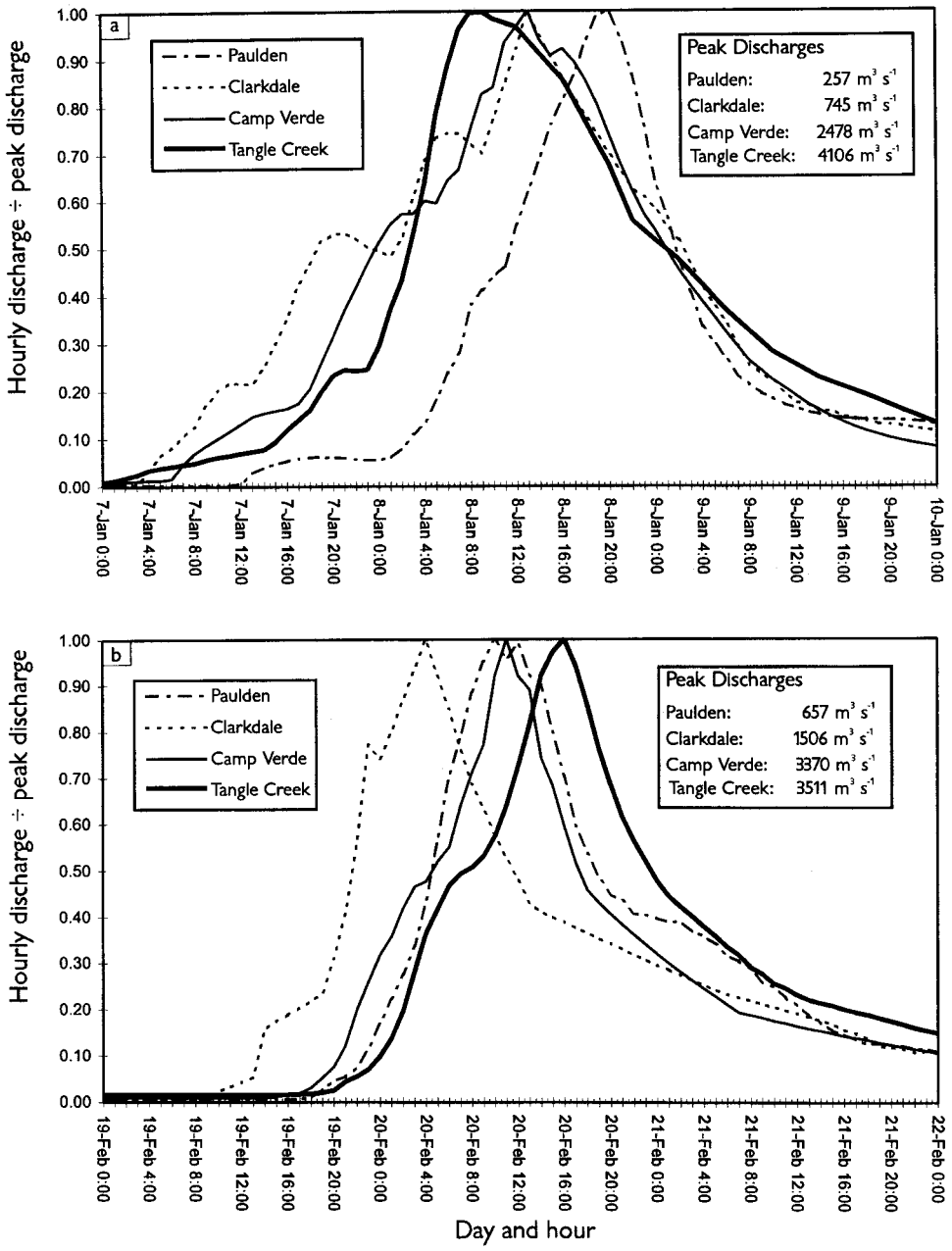

Figure 13. Normalized hydrographs from gauging stations on the Verde River, a, January 7–9; b, February 19–21. Based on data in Smith et al., (1994) and provisional data from the U.S. Geological Survey.

more extreme than those in the watershed of Oak Creek (which is 25% smaller than Sycamore Canyon).

These differences in the timing of flood peaks indicate that in both the early January and late February events, less than 50%, and perhaps as little as 25%, of the basin contributed to the peak discharges recorded at the Tangle Creek gauge. In the case of the January event, runoff delivered from the entire basin eventually contributed to an immense volume of runoff, but in the late February case, the delivery of runoff was much more limited in space and time, so the flow duration and total volume were considerably lower at the Tangle Creek gauge. It is clear from the basis of these two events that a larger flood could be generated under more optimal flood-enhancing circumstances in the Verde River Basin. Paleoflood hydrology provides a framework from which to address the possibility for larger floods by directly examining evidence for them in the geological record.

PALEOHYDROLOGICAL CONTEXT OF THE 1993 FLOODS

Paleoflood hydrology is a geological approach to the study of the magnitude and frequency of large floods that occurred prior to, or in absence of, systematic observation (Baker, 1987,

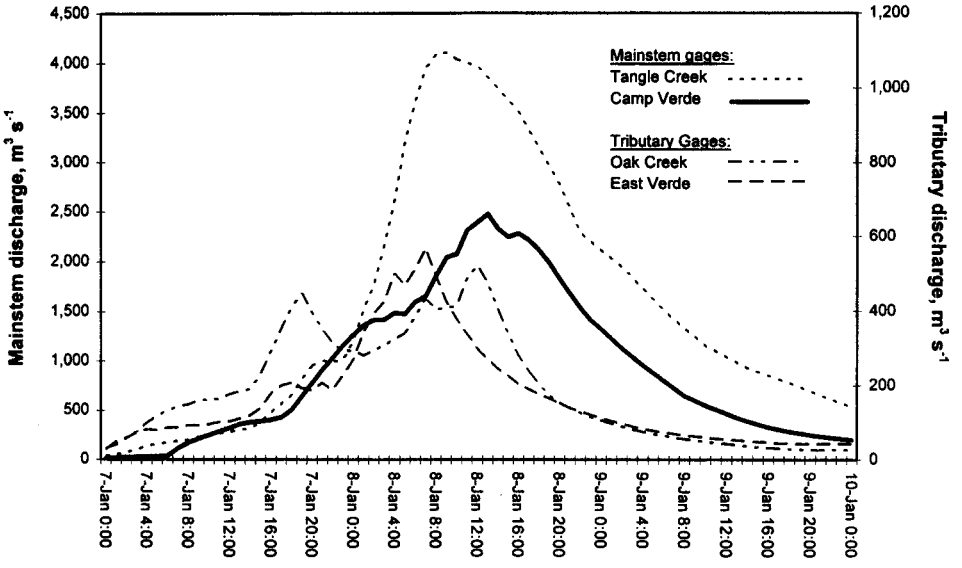

Figure 14. Comparison of mainstem Verde River flood hydrographs with tributary stream flood hydrographs, January 7–10, 1993. Based on data in Smith et al., (1994) and provisional data from the U.S. Geological Survey.

1989; Costa, 1987a). Extensive paleoflood research has been carried out in Arizona, and much of the paleoflood data from rivers throughout the state has been combined to establish a regional paleoflood chronology that spans 5,000 yr (Ely, 1992; Ely et al., 1993). This wealth of paleohydrological data provides a unique opportunity to evaluate the 1993 events in the context of the Holocene history of flooding in central Arizona.

Much of the Arizona paleoflood data has been obtained using the slackwater deposit–paleostage indicator (SWD-PSI) method (Baker, 1987, 1989). This approach involves relating geological evidence for extreme flooding in bedrock canyons to discharge-dependent water surface profiles calculated from a fixed boundary hydraulic model (O'Connor and Webb, 1988). The primary types of geologic evidence for flooding are flood slackwater deposits (SWD), which consist of sand and silt that accumulate in areas of markedly reduced flow velocities during large floods. In many bedrock canyons, deposits from the largest floods are often found in areas protected from low and moderate flood events, where they can persist for hundreds to thousands of years, particularly in arid and semiarid climates (Kochel and Baker, 1988). Age estimates can be obtained for individual deposits using radiocarbon dating techniques on organic material within or between them or with age constraints based on the presence of diagnostic archaeological artifacts. The presence of multiple deposits in a stratigraphic sequence allows for a relative age relationship between deposits to be determined. Paleoflood stages inferred from SWDs can be reinforced or augmented with other types of paleostage indicators (PSIs) including relict high-water marks such as flotsam lines, flood-scoured hill slopes, and flood-damaged vegetation.

SWD-PSI paleoflood studies are suited only to bedrock canyons because stable boundary conditions are assumed in the modeling, and only in such environments can flood deposits persist for long periods of time and retain their original relationship to the stream channel. On the Verde River, the relation between SWDs from the 1993 floods and the stratigraphy of older flood SWDs has been investigated in such a canyon setting.

Paleohydrological context of the 1993 floods in the Verde Basin

SWD-PSI paleoflood studies on two reaches of the Verde River between the Camp Verde and Tangle Creek gauge sites have produced a detailed, well-constrained paleoflood chronology that spans more than 1,000 yr (Ely and Baker, 1985; O'Connor et al., 1986). Post-1993 flood investigations of the SWD stratigraphy at selected sites in these reaches have provided valuable information regarding the relative magnitude of the 1993 event in the context of this long record of flooding (House, 1996; House et al., 1995). The stratigraphic column shown in Figure 15 is a schematic depiction of a trench in a sequence of flood deposits examined in June 1993. The trench is in an isolated alcove well protected from low- and moderate-magnitude floods along the river. This new site supplements a previous paleoflood study of this reach by O'Connor et al. (1986). Our interpretation of the stratigraphy incorporates evidence specific to this site combined with inferences derived from well-described flood stratigraphy from the paleoflood site downstream (Ely and Baker, 1985). Age designations shown in the figure are taken from those determined for deposits at the downstream reach that we infer to be correlative. Our inference is supported by examination of the downstream sites following the floods and the observation of similar relationships between individual flood deposits and their associated flood magnitude estimates.

The discharges reported in Figure 15 are from a rating curve for this site that was derived from step-backwater model-

ing of a 500-m (1,640-ft) reach of the river (House, 1996; House et al., 1995). The 1993 peak discharge through the reach is well constrained by records from the Camp Verde gauge (upstream) and the Tangle Creek gauge (downstream). The paleoflood discharges are based on the corresponding SWD elevations and have been adjusted upward to reflect the difference between the heights of diagnostic peak stage indicators (flotsam) and SWDs from the largest 1993 flood at this site (House et al., 1995).

The uppermost deposit in the section is probably correlative to the uppermost deposit at the downstream site based on stratigraphic relations and comparable discharge estimates. At the downstream site, the maximum age of the deposit has been estimated to be approximately 1000 B.P. based on diagnostic archaeological artifacts found on the surface and a radiometric date of in situ charcoal (Ely and Baker, 1985). The underlying unit (unit 2) predates unit 1 by an unknown amount. Unit 2 is separated from unit 4 by a layer of hillslope colluvium, which suggests a relatively long hiatus in flood deposition; the lack of any absolute age control, however, precludes any age designation more specific than that it is older than unit 1. Unit 3 is interpreted as a deposit inset into the colluvial unit separating units 2 and 4. Based on similarities in stratigraphic relationships and discharge estimates from the downstream site, this unit is inferred to be from the 1891 flood. However, this correlation is tenuous. Unit 5 is the deposit from the largest of the 1993 floods at this site. Its stratigraphic relationship

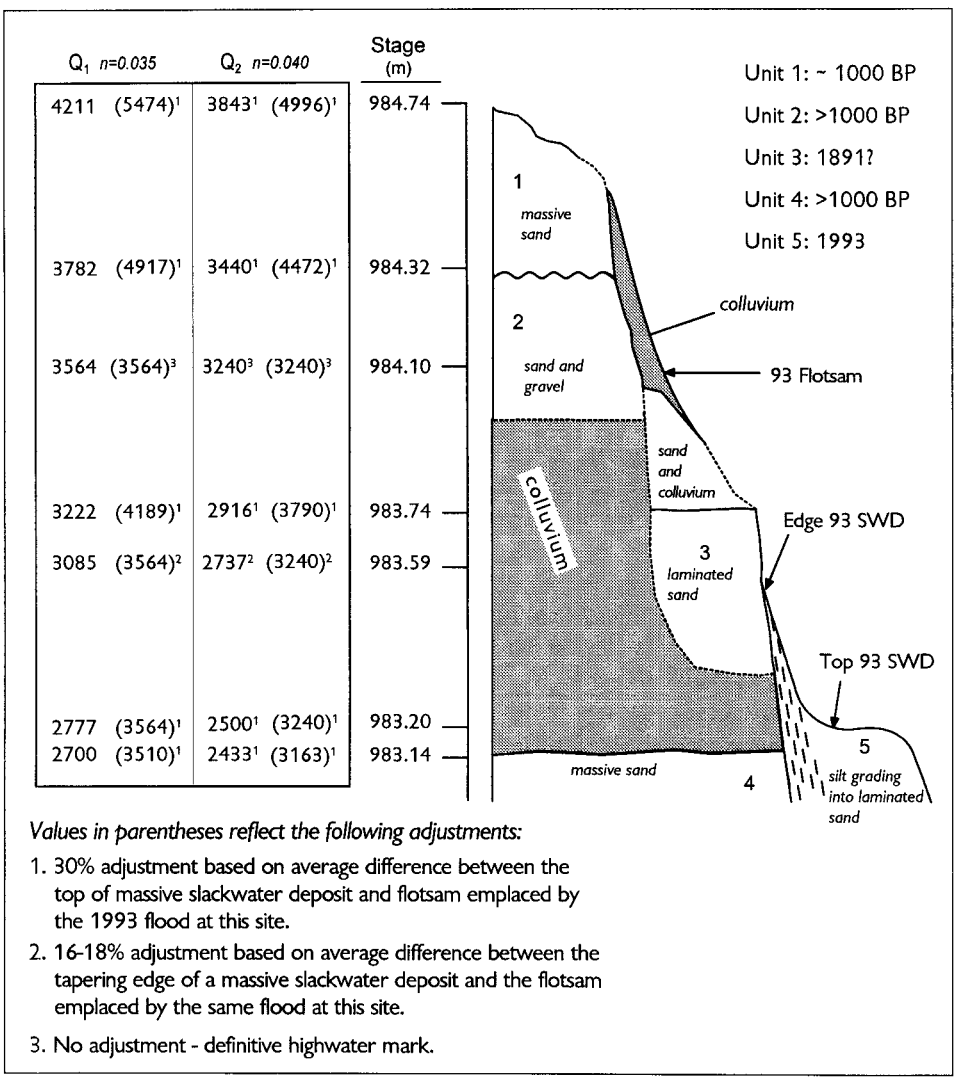

Figure 15. Schematic depiction of flood slackwater deposit (SWD) stratigraphy at the paleoflood site discussed in the text. Discharges shown at left (Q_1 and Q_2) are from step-backwater modeling of a 500-m (1,640-ft) reach of the river using two different estimates of channel roughness (n). Discharges reflect correction for differences in flood stage inferred from different types of highwater marks (flotsam versus slackwater deposits) from the largest 1993 flood at this site. Several tributaries that enter the river between this site and the gauge below Tangle Creek experienced significant flooding in the winter of 1993 (see House et al., 1995, for detailed discussion).

to the rest of the sequence is obvious. We note that the dramatic increase in discharge of the early January flood between Camp Verde and Tangle Creek was such that the peak discharge was less than that of the late February flood at this site (House, 1996; House et al., 1995). However, as a result of the dramatic increase in flood discharge described previously, the early January flood was the largest at sites farther downstream.

In the flood stratigraphy at this site there is evidence for at least five large floods. Three are larger than the 1993 flood; of these, two occurred prior to 1000 B.P., and one occurred slightly more than a century ago (probably in 1891). The two oldest floods were considerably larger than the 1993 event, whereas the 1993 event and the inferred 1891 event were similar in magnitude. The magnitude of the 1891 flood in the vicinity of the Tangle Creek gauge is estimated to be only slightly larger than the 1993 flood, which is consistent with our stratigraphic interpretation and that of Ely and Baker (1985). There is also evidence at this site for a flood that was slightly smaller than the 1993 flood, which must have occurred prior to 1000 B.P. (unit 4).

Regional peak flood magnitude characteristics

Combining the regional paleoflood data with all gauged and historical flood discharge data from Arizona (including the record-breaking 1993 peaks) illustrates an interesting relationship in regional flood magnitude–drainage area relationships. The plot shown in Figure 16 depicts the largest gauged, historical, and paleoflood discharges for drainage basins of varying area in the Lower Colorado River Basin (see Enzel et al., 1993). An envelope curve delimits the maximum values of the data spread. The position of the curve is based only on gauged and historical flood data (including U.S. Geological Survey indirect estimates from miscellaneous sites). The addition of the paleoflood values to the plot effectively extends the temporal base of the data set in real time, in some cases by hundreds to thousands of years. Because all of the paleoflood values fall on or very near the curve, it has been proposed as a reasonable approximation of a natural upper bound on flood magnitudes in this region that has persisted for the last several thousand years (Enzel et al., 1993).

Comparing the 1993 record flood peaks to this figure provides an interesting perspective on the relative magnitude of this major winter flooding episode. From this comparison, it is clear that many individual flood peaks in 1993 were quite large, but all were within the realm of documented natural tendencies of extreme floods in the region, as the Verde River paleoflood data attest. Some flood peaks from the larger basins were relatively close to the envelope, whereas record floods in basins less than about 1,000 km^2 (~400 mi^2) were small in relation to the curve, because extreme floods in small basins within the region usually result from localized, intense thunderstorms. The plot also indicates that basins without paleoflood records experienced floods comparable to, and in some cases larger than, the largest paleofloods recorded in basins of similar sizes.

DISCUSSION

The immense regional scale of the 1993 flooding episode is encapsulated in Figure 16. Considering the regional scale and the magnitude of individual events in the largest basins, we contend that the anomalous hydroclimatological conditions that characterized the 1993 floods are probably analogous to those associated with most of the large paleofloods in the largest basins. The sequence of events culminating in the 1993 flood episode illustrates that certain hydroclimatological phenomena are extremely conducive to the generation of huge floods on large rivers in Arizona, particularly in the Central Highlands Province. These phenomena include abnormally high rainfall totals throughout the region, repeated accumulation and melting of heavy snowpack, direct rainfall on snowpack, and prolonged periods of relatively moderate intensity rainfall over large areas and of high intensity rainfall over smaller areas. Each of these processes in 1993 was initiated and perpetuated by a persistent, anomalous circulation pattern that repeatedly steered alternately warm and cold storms into the region along a southerly displaced storm track over a three-month period. The scale of these phenomena was such that streams throughout much of the state experienced severe flooding.

Evidence for larger floods in the paleoflood record thus suggests more extreme variations on the hydroclimatic scenario played out in 1993. Furthermore, optimal basinwide timing of flood runoff coming from a similar set of circumstances might also produce events large enough to have emplaced the paleoflood deposits. Recall that a larger peak on the Verde River might have occurred in January 1993 were it not for relatively slight variations in the timing of precipitation and runoff in different portions of the basin.

In a summary treatment of paleoflood chronologies from the southwestern United States, Ely (1992) and Ely et al., (1993) proposed that there is an indication of temporal clustering of large floods that is consistent with evidence of hydrological variability inferred from other types of proxy indicators of regional climate change over the last 5,000 yr. The periods of apparent clustering defined by Ely et al. (1993) were determined by stratigraphic evidence (SWDs) of approximately synchronous regional flooding. Their analysis suggested that the timing of clusters of large floods corresponds to periods of transitions in the regional climate. The interpretation of the 1993 floods in the context of regional hydroclimatological phenomena stemming from global circulation characteristics offers important insights into the physical basis of flood clustering in the paleorecord in the southwestern United States.

The 1993 flood scenario provides a convincing modern analogue for the processes that probably operated to generate comparably large paleofloods. Hence we suggest that clusters of flooding in the paleorecord of the Southwest are best explained by a global circulation scenario involving an unusually high frequency of winters characterized by a southerly displaced Pacific storm track enhanced by subtropical flow. The key factor in this scenario is the development of a circulation anomaly in the eastern North Pacific Ocean that promotes the formation of a split flow in the westerlies

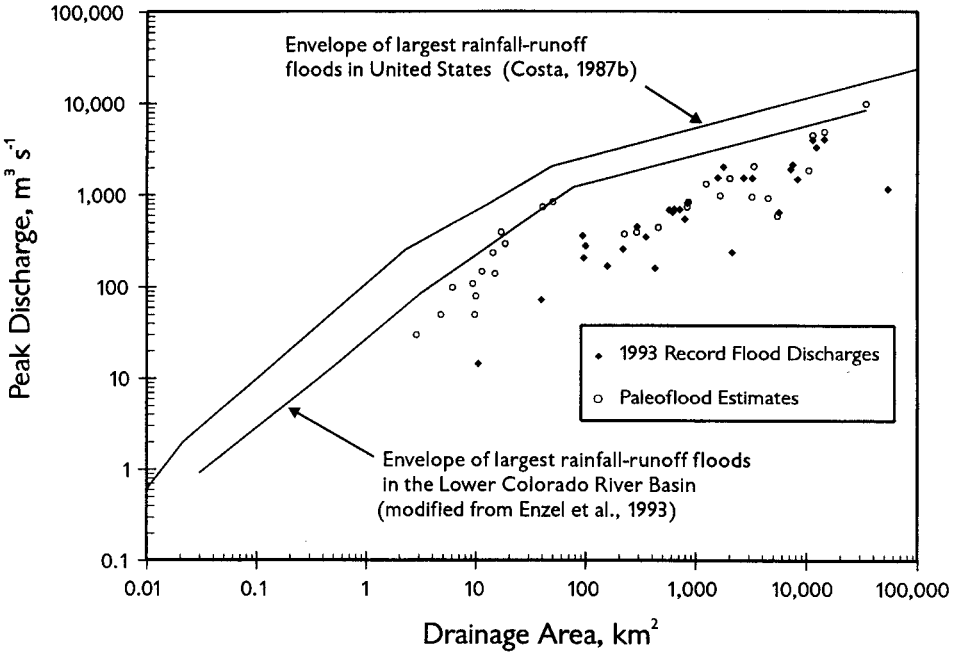

Figure 16. Comparison of the 1993 record flood peaks from unregulated basins to paleofloods and the envelope curve of the maximum gauged and historical floods in the lower Colorado River basin. Envelope curve slightly modified from Enzel et al., (1993). Also shown is the envelope curve for the largest floods in the United States as of 1987 (Costa, 1987b).

and forces the southern branch of the normal Pacific storm track to lower latitudes. Such a winter pattern has been associated with ENSO conditions over the last 100+ yr (e.g., in the winters of 1890–1991, 1964–1965, 1979–1980, 1992–1993, 1993–1994) but might also develop independent of an El Niño in response to other kinds of global circulation changes.

CONCLUDING REMARKS

We have shown that the 1993 Arizona flood sequence was comparable in terms of regional scale and individual flood magnitudes to the largest-known flooding episodes in this region over at least the last 1,000 yr, and possibly as long as the last 5,000 yr. The 1993 episode resulted from a distinctive combination of hydroclimatological and hydrological events. During the middle and late Holocene, such events have characterized periods of climatic transition, both regionally and globally (Ely et al., 1993). Taken in the context of the paleoflood record and its connection to regional hydroclimatological phenomena, characteristics of the 1993 flood episode are remarkably consistent with documented regional trends in the temporal variability of extreme flooding in the southwestern United States.

We have identified the winter season conditions of atmospheric circulation on global, hemispheric, and regional scales that resulted in significant and persistent flooding in Arizona during 1993. ENSO-related ocean-atmosphere interactions supported the development of an atmospheric circulation anomaly in the eastern North Pacific Ocean that included a blocking high-pressure pattern over the Gulf of Alaska. An associated split jet stream deflected the storm track southward across the southwestern United States and directed a long sequence of significant winter storms across Arizona.

We have also established the paleohydrological context of the 1993 floods along the Verde River by comparing their sedimentological evidence with similar evidence from comparably large and even larger floods that have occurred over the past 1,000 yr. We conclude that the anomalous hydroclimatological conditions associated with the 1993 floods are characteristic of the types of conditions that were required to generate the floods of comparable or greater magnitude that are evident in the paleoflood record.

The paleoflood record on the Verde River indicates that, although the 1993 floods were rare and extreme events, they were not unprecedented. This unique information is afforded only by the geological evidence, and it should serve as a clear reminder that such extreme events are inevitable outcomes of natural processes. Similar occurrences in the future are certain. Knowledge of the hydroclimatological and paleohydrological context of the 1993 Arizona flood sequence can serve as a tool for flood hydrologists, water supply managers, and floodplain managers to better understand the physical processes associated with extreme floods and their inherent patterns. An enhanced understanding could lead to better management policies and better water-supply forecasting and reservoir management over both the long and short terms as well as a greater ability to foresee local consequences of regional and global climatic phenomena.

ACKNOWLEDGMENTS

Many people helped in the preparation of this manuscript. We owe particular thanks to Chris Smith of the USGS, Tucson, for allowing free access to the USGS hydrological data base. Steve Waters of the Maricopa County Flood Control District and Dallas Reigle of the Salt River Project provided supplementary precipitation data. Michelle Wood and Fenbiao Ni of the Tree-Ring Laboratory, University of Arizona, compiled the flood hydroclimatology and atmospheric circulation data and prepared several figures. Pete Corrao and Carrie House helped with preparation of many figures. We are grateful to Vince Cronin of the University of Wisconsin, Milwaukee, for his thoughtful and comprehensive review of the manuscript. This research was supported in part by the Salt River Project, Arizona; the Arizona Geological Survey; the Quaternary Sciences Center of the Desert Research Institute; the Hydrological Sciences Program of the National Science Foundation, grant EAR-9305252; the U.S. Geological Survey Water Resources Research Grant Program, award # 14-08-0001-G1754; the Climate and Global Change Program of the National Oceanic and Atmospheric Administration, grant GC94-504; and the National Institute for Global Environmental Change–Western Regional Center, Research Agreement No. W/GEC 92-020. This manuscript is part of the senior author's doctoral dissertation and is contribution #41 from the Arizona Laboratory for Paleohydrological and Hydroclimatological Analysis (ALPHA), Department of Geosciences, University of Arizona.

REFERENCES CITED

Baker, V. R., 1987, Paleoflood hydrology and extraordinary flood events: Journal of Hydrology, v. 96, p. 79–99.

Baker, V. R., 1989, Magnitude and frequency of paeleofloods, *in* Beven, K., and Carling, P., eds., Floods: Hydrological, sedimentological, and geomorphological implications: New York, John Wiley, p. 171–183.

Bell, G. D., and Basist, A. N., 1994, The global climate of December 1992–February 1993. Part I: Warm ENSO conditions continue in the tropical Pacific; California drought abates: Journal of Climate, v. 7, p. 1581–1605.

Chin, E. H., Aldridge, B. N., and Longfield, R. J., 1991, Floods of February 1980 in southern California and central Arizona: U.S. Geological Survey Professional Paper 1494, 126 p.

Costa, J. E., 1987a, A history of paleoflood hydrology in the United States: 1800–1970, *in* Landa, E. R., and Ince, S., eds., The history of hydrology, history of geophysics, v. 3: Washington, D.C., American Geophysical Union, p. 49–53.

Costa, J. E., 1987b, A comparison of the largest rainfall-runoff floods in the United States with those of the People's Republic of China and the world: Journal of Hydrology, v. 96, p. 101–115.

Ely, L. L., 1992, Large floods in the southwestern United States in relation to late Holocene climatic variations [Ph.D. thesis]: Tucson, University of Arizona, 326 p.

Ely, L. L., and Baker, V. R., 1985, Reconstructing paleoflood hydrology with slackwater deposits: Verde River, Arizona: Physical Geography, v. 6, p. 103–126.

Ely, L. L., Enzel, Y., Baker, V. R., and Cayan, D. R., 1993, A 5000-year record of extreme floods and climate change in the southwestern United States: Science, v. 262, p. 410–412.

Ely, L. L., Enzel, Y., and Cayan, D. R., 1994, Anomalous north Pacific atmospheric circulation and large winter floods in the southwestern United States: Journal of Climate, v. 7, p. 977–987.

Enzel, Y., Ely, L. L., House, P. K., Baker, V. R., and Webb, R. H., 1993, Paleoflood evidence for a natural upper bound to flood magnitudes in the Colorado River Basin: Water Resources Research, v. 29, p. 2287–2297.

Guttman, N. B., Lee, J. J., and Wallis, J. R., 1993, Heavy winter precipitation in southwest Arizona: Eos (Transactions, American Geophysical Union), v. 74, p. 482–485.

Hirschboeck, K. K., 1985, Hydroclimatology of flow events in the Gila River Basin, central and southern Arizona [Ph.D. thesis]: Tucson, University of Arizona, 335 p.

Hirschboeck, K. K., 1987, Hydroclimatically-defined mixed distributions in partial duration flood series, *in* Singh, V. P., ed., Hydrologic frequency modeling: Boston, D. Reidel Publishing, p. 199–212.

Hirschboeck, K. K., 1988, Flood hydroclimatology, *in* Baker, V. R., Kochel, R. C., and Patton, P. C., eds., Flood geomorphology: New York, John Wiley & Sons, p. 27–50.

House, P. K., 1993, The Arizona floods of January and February 1993: Arizona Geology, v. 23, p. 1–9.

House, P. K., 1996, Reports on applied paleoflood hydrological investigations in western and central Arizona [Ph.D. thesis]: Tucson, University of Arizona, 356 p.

House, P. K., Pearthree, P. A., and Fuller, J. E., 1995, Hydrologic and paleohydrologic assessment of the 1993 floods in the Verde River, central Arizona: Arizona Geological Survey Open-file Report 95-20, 23 p.

Huckleberry, G. A., 1994, Contrasting channel response to floods on the middle Gila River, Arizona: Geology, v. 22, p. 1083–1086.

Kochel, R. C., and Baker, V. R., 1988, Paleoflood analysis using slackwater deposits, *in* Baker, V. R., Kochel, R. C., and Patton, P. C., eds., Flood geomorphology: New York, John Wiley & Sons, p. 357–376.

MacNish, R. D., Smith, C. F., and Goddard, K. E., 1993, Floods in Arizona, January 1993: U.S. Geological Survey Open-File Report 93-54, 2 p.

National Oceanic and Atmospheric Administration, 1992, Arizona, *in* Climatological data (U.S. Department of Commerce), December 1992, v. 96, n. 12, p. 6–8.

National Oceanic and Atmospheric Administration, 1993a, Arizona, *in* Climatological data (U.S. Department of Commerce), January 1993, v. 97, n. 1, p. 6–8.

National Oceanic and Atmospheric Administration, 1993b, Arizona, *in* Climatological data (U.S. Department of Commerce), February 1993, v. 97, n. 2, p. 6–8.

O'Connor, J. E., and Webb, R. H., 1988, Hydraulic modeling for paleoflood analysis, *in* Baker, V. R., Kochel, R. C., and Patton, P. C., eds., Flood geomorphology: New York, John Wiley & Sons, p. 393–402.

O'Connor, J. E., Fuller, J. E., and Baker, V. R., 1986, Late Holocene flooding within the Salt River Basin, central Arizona: Unpublished report to the Salt River Project, Tempe, Arizona, 60 p.

Patterson, J. L., and Somers, W. P., 1966, Magnitude and frequency of floods in the United States. Part 9: Colorado River Basin: U.S. Geological Survey Water-Supply Paper 1683, 476 p.

Roeske, R., Garrett, J., and Eychaner, J., 1989, Floods of October 1983 in southeastern Arizona: U.S. Geological Survey Water-Resources Investigations Report 85-4225-C, 77 p.

Sellers, W. D., and Hill, R. H., 1974, Arizona climate, 1931–1972: Tucson, University of Arizona Press, 616 p.

Smith, C. F., Rigas, P. D., Ham, L. K., Duet, N. R., and Anning, D. W., 1994, Water resources data, Arizona, Water year 1993: U.S. Geological Survey Water-Data Report AZ-93-1, 360 p.

U.S. Army Corps of Engineers, 1994, Flood damage report, State of Arizona, floods of 1993: U.S. Army Corps of Engineers, Los Angeles District, South Pacific Division, 107 p.

Webb, R. H., and Betancourt, J. L., 1992, Climatic variability and flood frequency of the Santa Cruz River, Pima County, Arizona: U.S. Geological Survey Water-Supply Paper 2379, 40 p.

MANUSCRIPT ACCEPTED BY THE SOCIETY JANUARY 29, 1997

Printed in U.S.A.